QoS Aware Joint Observer and Networked PI/PID Controller Design using LMIs under Specified Rate of Packet Dropouts

Kaushik Halder[1], Saptarshi Das[2,3,*], Deepak Kumar Panda[2], Sourav Das[4], Amitava Gupta[4]

1) Department of Mechanical Engineering Sciences, University of Surrey, Guildford GU2 7XH, UK (e-mail: k.halder@surrey.ac.uk).
2) Department of Mathematics, College of Engineering, Mathematics and Physical Sciences, University of Exeter, Penryn Campus, Cornwall TR10 9FE, UK. (e-mail: saptarshi.das@ieee.org, dp457@exeter.ac.uk).
3) Institute for Data Science and Artificial Intelligence, University of Exeter, Laver Building, North Park Road, Exeter, Devon EX4 4QE, UK.
4) Department of Power Engineering, Jadavpur University, Salt Lake Campus, Kolkata 700098, India (e-mail: das_sourav@live.in, amitava.gupta@jadavpuruniversity.in).

Phone: +44-7448572598.

***Abstract*—This paper develops a novel formulation for quality of service (QoS) aware networked observer and PI/PID controller design in the presence of specified rate of random packet dropouts. We here derive the stability conditions for the controller and observer gains using asynchronous dynamical system (ADS) formulation of the networked control system (NCS) in discrete time which yields a set of linear matrix inequalities (LMIs). The control design has been validated on two test-bench energy systems viz. battery with DC/DC converter and synchronous generator with power system stabilizer. Numerical simulations report the joint observer and controller's performance in the presence of random packet drops within output feedback control scheme using PI/PID controllers and employing state estimation for the battery and synchronous generator systems. The major numerical challenge includes handling nonconvex constraints in LMIs and stabilizing the observer-based controller with specified rate of packet dropouts. Monte Carlo simulations are provided to compare the uncertain state trajectories, state estimation errors and control efforts under different probability of packet dropouts for the two test-bench energy systems.**

***Keywords*—Lyapunov stability; networked control system (NCS); observer; proportional integral derivative (PID) controller; linear matrix inequality (LMI); packet dropout**

1. INTRODUCTION

1.1. Background and Problem Definition

NCS has emerged as a sub-discipline of control theory which bridges the gap between stability derivations with packet dropouts and random delays [1]. Many well-tuned control systems may show unacceptable and even unstable closed loop response in the presence of random packet drops and/or communication delays, depending on the quality of the communication medium. This is even more challenging when only partial observations of the state variables in a higher order system are available for which one need to use an observer or state estimation algorithm to design a state feedback controller [2]. This is due to the fact that the inclusion of an observer in the control loop increases the order of the overall closed loop system [3]. Moreover, both the observer and PI/PID controller need to be designed together as an integrated framework for guaranteeing closed loop stability in order to handle a specified rate of random packet dropouts or the quality of service or QoS within NCS which is quite challenging and the main contribution of this paper. In NCS, different control loop components are usually spatially distributed i.e. sensors, actuators, controllers, etc. reside on different computer nodes and are connected through a shared real-time communication network in order to overcome the disadvantages of traditional point-to-point digital control systems, such as high design and implementation cost, difficulty in diagnostics and maintenance [4], [5]. The presence of unreliable shared communication network mostly causes random packet-drops and network induced delays in NCS. Therefore, it is quite challenging to analyze the stability and achieve acceptable control performances in the NCS under such scenarios i.e. packet-drops and communication delays.

1.2. Previous Works on Modelling of NCS and Effects of Unreliable Communication

Several researchers have attempted to analyze either only the stability or both stability and closed loop performance of NCS considering random packet-drops [6], random delays [7] and both [8]. Most of these approaches have formulated the NCS as a switched system [6], asynchronous dynamical system or ADS [9] and lifted model [10], [11], [12] and have used LMI technique [13] to design the controller for analyzing the stability and performance of the NCS loop. Again, in order to analyze the stability and performance of NCS, observer based output feedback controller design has been attempted by several researchers under packet dropout [6], communication delays [14] or both scenarios [15]. The approach proposed in [4], [6] used the switched system approach to design NCS under random packet-drop condition and analyzed the stability of NCS under such a scenario using observer based output feedback controller. In [16], an observer-based H_∞ output feedback controller has been designed for NCS with parametric uncertainties, dynamic quantization and random packet drops. Instead of joint observer-based controller design, separate approaches for filter design [17], [18] and controller design [19] for NCS under network constraints were

proposed in the presence of dynamic quantization, packet drops, communication delays etc. For example, H_∞ filter [18] and fuzzy peak-to-peak filter [20] have been designed for NCS under random packet drops. An estimator has been designed for switched complex dynamical network under quantization in [21], whereas memory based sampled data control [19] and event trigger control scheme [22] were proposed for semi-Markov jump complex dynamic network system under network transmission delay. However, these methods may not be easily extendable for controllers with memory like the PI/PID structure with memory elements i.e. integrator and differentiator terms and with observers which the present paper aims to tackle. Few attempts has also been made for designing delay dependent LMIs for PI controlled NCS using Lyapunov Krasovskii functional in [23].

In this paper, we have modeled the NCS as an ADS. Since most of the industrial output feedback control schemes use PID controllers [24], recent attention has been focused more towards designing PID controllers for NCS applications to retrofit the existing PID control loops using a robust design framework to ensure stability for unreliable communications. However very few works have attempted designing PI/PID controllers considering both stability and performance analysis for NCS under random packet drops and/or delays. Amongst previous attempts, stability analysis of NCS with existing PID controller gains under packet-drops and/or variable delays (jitter) are notable, by modeling the NCS as switched system [25], [26]. Another approach presented in [10], [27] assumes a time-driven sensor with a dual rate event-driven PID controller for an NCS under network induced delay. As the sensor is time-driven, it sends the data to the controller in every sampling instant. The controller also being time-driven generates data at faster rate and the controller will start generating the output only on the arrival of the sensor data which may induce a sensor to controller delay (τ_{sc}). Depending on the delay, some initial control actions may not be possible to compute and hence cannot be applied to the plant. The methodology presented in [10], [27] only considers round trip time (RTT) delay instead of packet dropouts. The consequences arising from varying delay has also been tackled by adopting a dual-rate approach.

1.3. Previous Works on Networked Controller Design

In [28], [29], [30] optimization techniques are used by minimizing different cost functions in order to find optimal parameters of PID controllers in NCS. For example, Pan *et al.* [30] have tuned fractional order PID controllers using evolutionary algorithms for challenging plants like open loop unstable systems with random packet drops and time delays in NCS by minimizing a custom cost function of control loop error and controller effort. In [31], PI/PID controllers have been tuned using gain and phase margin specifications for first/second-order plus dead time processes under the effect of network induced delays. In addition to the above approaches, LMI techniques are also broadly used to design robust controllers for NCS. For example, Zhang *et al.* [32], [33] have considered event-driven PID controller as a static output feedback (SOF) controller and have obtained the PID controller gains using LMIs under networked induced delays and packet drops. As opposed to these previous works, this paper derives the observer and PI/PID controllers for a specified QoS or rate of packet drop and also does not consider an existing PI/PID controller gains unlike Dasgupta *et al.* [25], [26] since the controller gains should be adaptable to the need of the QoS to avoid under-specification or over-specification of the control performance. This paper also does not consider metaheuristic swarm and evolutionary optimization based optimal tuning of PI/PID or state feedback controller gains for NCS under packet drop scenario as in Pan *et al.* [30], [34], [35] and Panda *et al.* [36], since such simulation based brute-force control design approach may not always guarantee closed loop stability under random packet drops since it can be better modelled in the switched system framework although in a more conservative setting for a specified probability of packet drop. On contrary, this paper first designs an observer to estimate unmeasured states and then uses the observed states to construct the estimated output signal considering the network induced distortions. The PI/PID controller and observer gains are designed jointly within the LMI framework which gives deterministic solution with guaranteed Lyapunov stability for a fixed probability of packet drops.

Over past decades [5], design of SOF controllers [37], [38] and reduced order controllers [39] become very popular research area in NCS, especially using LMIs with non-convex constraints. Due to the non-convex constraints in the problem formulation in NCS, they become NP-hard as explained in [40]. Hence, exponentially long time will be required to get solutions of these problems and global convergence is not always ensured. To counter these problems, several alternative approaches were proposed. As an example, predictive controller has been designed in [41] for an NCS subjected to random packet drops by formulating LMIs and using non-dominated sorting genetic algorithm-II (NSGA-II) to find the global solution for simultaneous minimization of multiple non-convex contradictory objectives which tunes optimal gains for predicted control signals to compensate for the effect of packet drops. As the evolutionary optimization was carried out in offline mode in [41], computational complexity and guaranteed convergence were not of major concern. Several other numerical approaches have been proposed to solve LMIs or bilinear matrix inequalities (BMIs) with non-convex constraints arising in NCS problems. For instance, cone complementarity linearization (CCL) algorithm was used in [37], [42] to solve LMIs with nonconvex constraints formulated from the analytical stability condition for NCS. Alternatively, BMIs arising in NCS with packet drops have been converted into a two stage LMI coupled with global metaheuristic optimization in Pan and Das [43] using a sub-optimal performance measure within a linear quadratic regulator (LQR) framework.

1.4. Novelty of This Paper

Here, an observer based discrete time PI/PID controller design approach has been proposed to control two test-bench energy systems within an NCS framework with random packet drops. Nowadays most of the efficient energy generation and conversion systems requires an open communication infrastructure and therefore, it is an open challenge to integrate distributed sensing,

communication, control and computing for efficient and real time operation of such industrial systems. However, there will be inevitable random communication delays and packet drops in the control loops due to the physical distance between the sensors, controllers and actuators [4], [5]. Previously, control laws for similar test-bench energy systems like DC/DC converters and synchronous generators under communication delays and packet drops have been designed in [44], [45] but without joint design of observer based controller with memory such as PI/PID structure. However, in large scale monitoring scenario in energy applications, measuring all important variables may not be feasible due to physical and engineering constraints. Therefore, it is important to incorporate observers which can estimate the unmeasured states and enhance monitoring and control performance of energy systems under random packet drops due to the unreliable network effects. To address these problems, the proposed solution and the contributions of this paper are as follows:

- Firstly, the NCS with observer-based PI/PID controller has been modelled as a switched system using ADS approach considering random switching between sensor to observer and controller to actuator that causes random packet drops in both feedback as well as forward path of the NCS as shown in Figure 1. Here, an observer is used to estimate the unmeasured states of the system in the presence of random packet drops. Then the system output computed from the observed state variables is used to design the time-driven PI/PID controller for the NCS under random packet drops.
- Secondly, Lyapunov stability criteria based LMI approach has been used here to design the observer, PI/PID controller gains which guarantee the exponential stability with the existence of a common quadratic Lyapunov function (CQLF) i.e. $\mathbf{P} = \mathbf{P}^T > \mathbf{0}$ [12], [25], [46], [47] for the NCS modelled as an ADS under random packet drops. This is achieved by satisfying the specified rate constraint (r) of effective transmissions or the packet drop probability or the QoS.
- Thirdly, stability conditions for this problem provides LMIs with nonconvex constraints which is being solved by converting it into a sequential optimization problem subjected to LMI constraints using the CCL algorithm [37], [42].

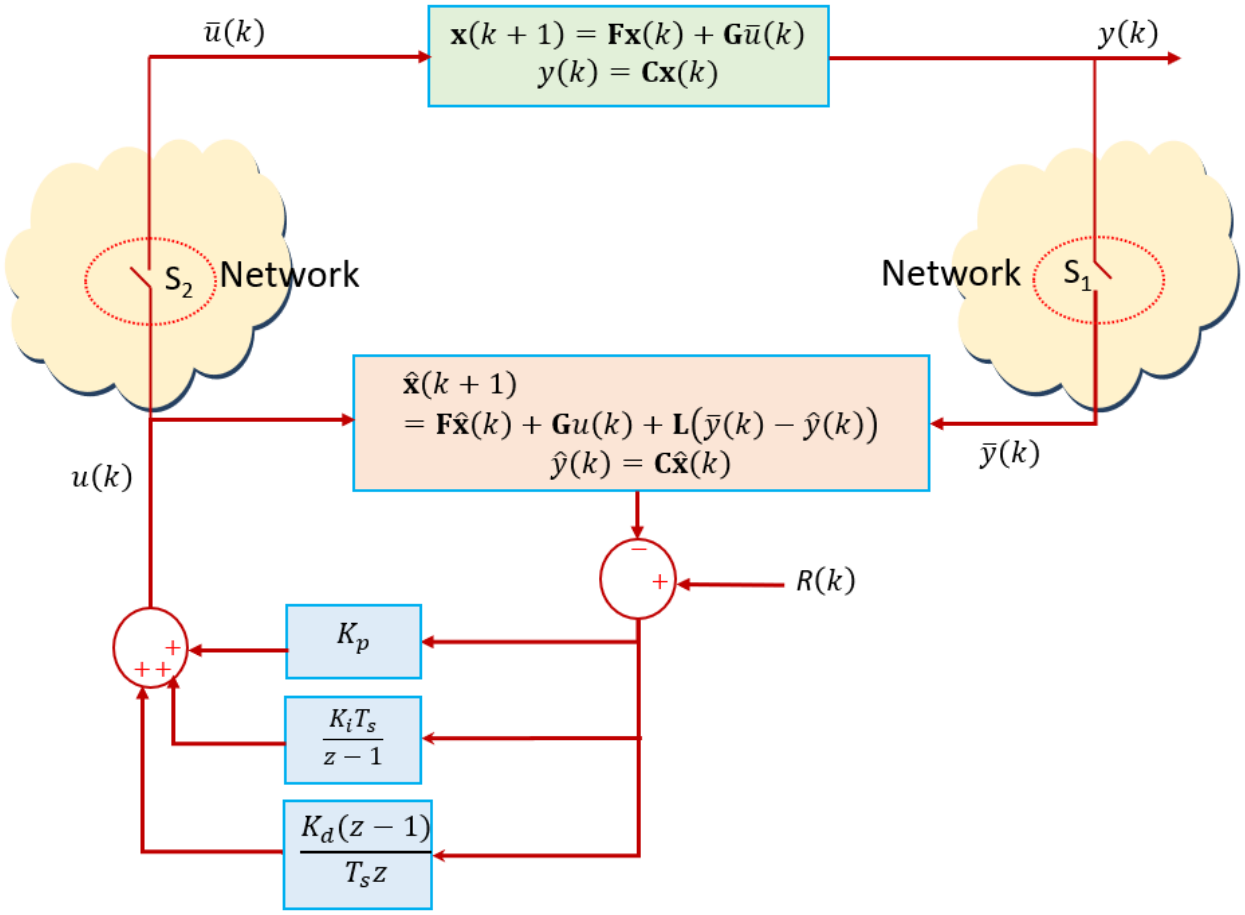

Figure 1: Networked observer based PID controller with packet drops in both the forward and feedback path to handle a linear discrete time system.

In this paper, we have not considered random delays in the NCS since delays greater than the sampling time can often be considered as a packet drop and helps in deriving the analytical stability derivations [48]. It is also to be noted that the methodology presented in this paper considers the design of PI/PID controllers and observer gains for any discrete time networked system under arbitrary rate of ineffective transmissions or packet drops. In this paper, the NCS is modelled as an ADS with fixed effective transmission rate r or the QoS which follows Bernoulli's distribution with two outcomes, either the packet being transmitted or dropped at each time instant.

2. MODELING OF NCS AS ADS UNDER PACKET DROPOUT

The schematic diagram of a single loop NCS is shown in Figure 1, where it is assumed that both the feedback (sensor to observer) as well as forward (controller to actuator) paths are connected through a shared communication medium or unreliable network. The effect of network in the feedback and forward path of an NCS can be represented by two switches $s_1(\bar{s}_1)$ and $s_2(\bar{s}_2)$, respectively which denote effective (ineffective) transmissions of packets. It is further assumed that a continuous time plant represented by a linear state space model is controlled by the discrete time PI/PID controller. Here the actuator has a zero-order hold (ZOH) at its input and a time driven sensor is placed at the system's output which operate with a sampling time T_s. Hence, the discrete time equivalent form of the continuous time system can be represented as:

$$\mathbf{x}(k+1)=\mathbf{F}\mathbf{x}(k)+\mathbf{G}\bar{u}(k),\ y(k)=\mathbf{C}\mathbf{x}(k), \tag{1}$$

where, $\mathbf{F}\in\mathbb{R}^{n\times n}$ is the system matrix, $\mathbf{G}\in\mathbb{R}^{n\times p}$ is the input matrix and $\mathbf{C}\in\mathbb{R}^{q\times n}$ is the output matrix, $\mathbf{x}(k)\in\mathbb{R}^n$, $\bar{u}(k)\in\mathbb{R}^p$ and $y(k)\in\mathbb{R}^q$ represent the states, system inputs or control/manipulated variables (after the network in the forward path) and outputs or process variables of a linear n^{th} order dynamic system.

Under the network environment in the multi path i.e. feedback and forward path of an NCS as shown in Figure 1, the plant (1) is either controlled by the observer:

$$\begin{aligned}\hat{\mathbf{x}}(k+1)&=\mathbf{F}\hat{\mathbf{x}}(k)+\mathbf{G}\bar{u}(k)+\mathbf{L}\left(\bar{y}(k)-\hat{y}(k)\right)\\ \hat{y}(k)&=\mathbf{C}\hat{\mathbf{x}}(k),\end{aligned} \tag{2}$$

based discrete time PI controller with the output signal:

$$u(k)=K_p\left(R(k)-\hat{y}(k)\right)+K_iT_s\sum_{i=1}^{k}\left(R(k)-\hat{y}(i)\right), \tag{3}$$

or by observer (2) based discrete time PID controller with the output signal:

$$u(k)=K_p\left(R(k)-\hat{y}(k)\right)+K_iT_s\sum_{i=1}^{k}\left(R(i)-\hat{y}(i)\right)+\frac{K_d}{T_s}\left(\left(R(k)-\hat{y}(k)\right)-\left(R(k-1)-\hat{y}(k-1)\right)\right), \tag{4}$$

where, $\mathbf{L}$ represents the observer gains and $\{K_p,K_i,K_d\}$ represent the proportional, integral and derivative gains of the PID controller and $\hat{\mathbf{x}}(k)\in\mathbb{R}^n,\hat{y}(k)\in\mathbb{R}^q$ are the observed states and the corresponding estimated output of the system respectively. Here, $\bar{y}(k)$ represents the system output after the network in feedback path and $R(k)$ represents the reference input. In Figure 1, the observer is constructed in a non-traditional way since it takes the control/manipulated variable $u(k)$ before the network in forward path while it takes the system output or process variable after the network in the feedback path i.e. $\bar{y}(k)$. The observer gain ($\mathbf{L}$) corrects the discrepancy between the distorted output after the network in feedback path and the estimated output ($\bar{y}(k)-\hat{y}(k)$). However, alternative design approaches could have considered the observer input as the control packets after the network in the forward path as well i.e. $\bar{u}(k)$ which may have changed the design framework. The reason behind such a choice is that under centralized control but decentralized sensing scheme in NCS, the controller and observers are usually located at a distant control center for smart grids and smart energy systems, far away from the actuators and the energy system being controlled [49]. Therefore, the observer is always unaware of the true system input after the network ($\bar{u}(k)$) and system output before the network ($y(k)$) which explains why the nearest observations i.e. control packets after the PI/PID controller ($u(k)$) and the distorted measurements or sensed process variables ($\bar{y}(k)$) should be used in the observer to estimate the system states. Also, it is to be noted in Figure 1 that the estimated states are next used to calculate an approximate system output ($\hat{y}(k)=\mathbf{C}\hat{\mathbf{x}}(k)$) which is then fed to the PI/PID controller rather than the available measurements after the network ($\bar{y}(k)$). This is due to the fact that for large probability of packet drops and in poor communication network conditions, such measurements may not be reliable to use for control purpose while the estimated output ($\hat{y}(k)$) is much close to the original unmeasurable output ($y(k)$) since the observer formulation was done specifically to reduce the effect of random distortions due to the network and estimate the original states and therefore the system output.

It has been shown later that depending on the structure and the memory elements of the controller (PI or PID), the NCS modeled as switched systems become very different and hence needs to be tackled separately. Now an NCS has been modeled with the discrete time plant (1) and a time-driven observer based discrete time PI (3) and PID (4) controllers as an ADS under random packet drop scenario using the approach reported in [46], [25] with the following assumptions:

- All the packets are time-stamped i.e. sampling instant at which it is sampled. The reference is taken as the timeline of the sensor.

- Controller and the actuator both are time-driven i.e. current time-stamped data are accepted and others are discarded.

From Figure 1, the following hold with $s_1(\bar{s}_1), s_2(\bar{s}_2)$ representing the Boolean variables corresponding to effective (ineffective) transmissions across the two switches S_1 and S_2 respectively:

$$\left.\begin{array}{ll} s_1: & \bar{y}(k)=y(k) \quad \text{for effective transmission} \\ \bar{s}_1: & \bar{y}(k)=\bar{y}(k-1) \quad \text{for ineffective transmission} \\ s_2: & \bar{u}(k)=u(k) \quad \text{for effective transmission} \\ \bar{s}_2: & \bar{u}(k)=\bar{u}(k-1) \quad \text{for ineffective transmission} \end{array}\right\}. \tag{5}$$

It is seen from (5) that four possible sub-systems can be formulated for an NCS modelled as an ADS under the Boolean combinations $(s_1,s_2),(\bar{s}_1,s_2),(s_1,\bar{s}_2)$ and $(\bar{s}_1,\bar{s}_2)$, where $(s_1,s_2),(\bar{s}_1,s_2),(s_1,\bar{s}_2)$ and $(\bar{s}_1,\bar{s}_2)$ describes four different cases i.e. no packet drop in both feedback and forward path, packet drop in feedback path only, packet drop in forward path only and packet drop in both feedback and forward path, respectively. The corresponding NCS can be represented as an ADS with rate constraint (r) or the QoS using the four sub-systems represented by $\tilde{\mathbf{\Phi}}_{\sigma(k)}, \sigma(k)=1,2,3,4$ and the reference input $R(k) = 0$ (in Figure 1) as:

$$\mathbf{z}(k+1)=\tilde{\mathbf{\Phi}}_{\sigma(k)}\mathbf{z}(k); \quad \sigma(k)=1,2,3,4, \tag{6}$$

where, $\mathbf{z}(k)$ represents the augmented state-vector as defined in the formulations below and $\{\tilde{\mathbf{\Phi}}_1,\tilde{\mathbf{\Phi}}_2,\tilde{\mathbf{\Phi}}_3,\tilde{\mathbf{\Phi}}_4\}$ represent four sub-systems of the NCS under no packet drop, drop in feedback path only, drop in forward path only and drop in both feedback and forward path, respectively. For the four different cases in (5) and both observer based PI/PID controllers, the stability analysis leads to different sub-systems $\tilde{\mathbf{\Phi}}_{\sigma(k)}, \sigma(k)=1,2,3,4$, which are derived next.

It is to be noted that the four subsystems in (6) represent different conditions or subsystems of the NCS under a switched system formulation and need to be solved together under a common stabilization framework, for an observer based PI/PID controller design. Effect of the shared communication network is represented by two switches s_1 and s_2 in the feedback and forward path respectively as in (5). Depending on the switching dynamics in either path of the NCS, the effective and ineffective transmissions can be described as s_1 and $\bar{s}_1$ which represent the 'open' and 'close' states of the switching dynamics, which defines the effective and ineffective transmissions across feedback path, respectively. Similarly, the effective and ineffective transmissions in the forward path are represented by the switching dynamics s_2 and $\bar{s}_2$ which are described in (5). Therefore, the NCS with observer-based PI/PID controller can be modelled as an ADS consisting of four sub-systems as in (6) using these four different switching conditions. However, the NCS in (6) with these four sub-systems will be exponentially stable if there exists common quadratic Lyapunov function which can be written in terms of symmetric positive definite matrix $\mathbf{P}$ with $\mathbf{P}=\mathbf{P}^T>\mathbf{0}$ for all sub-systems of the NCS (6) by solving a suitable LMI subjected to certain inequality constraints which are obtained from the Lyapunov stability criteria.

2.1 NCS with Observer based PI Controller

Depending on the switching dynamics of the two switches s_1 and s_2 in Figure 1 for the NCS with linear discrete time plant and observer based PI controller, four different cases are derived next.

Case 1: Under no-drop scenario i.e. $\{s_1,s_2\}$ where

$$\bar{y}(k)=y(k)=\mathbf{C}\mathbf{x}(k), \tag{7}$$

and the state estimation error is

$$\mathbf{e}(k)=\mathbf{x}(k)-\hat{\mathbf{x}}(k). \tag{8}$$

Using (3), the controller output becomes:

$$\bar{u}(k)=u(k)=-K_p\hat{y}(k)-K_iT_s\sum_{i=1}^{k}\hat{y}(i). \tag{9}$$

Now, using $\hat{y}(k)=\mathbf{C}\hat{\mathbf{x}}(k)$ in (9) yields:

$$\bar{u}(k)=-K_p\mathbf{C}\hat{\mathbf{x}}(k)-K_iT_s\mathbf{C}\sum_{i=1}^{k}\hat{\mathbf{x}}(i). \tag{10}$$

Substituting:

$$\tilde{u}(k)=K_iT_s\mathbf{C}\sum_{i=1}^{k}\hat{\mathbf{x}}(i)=K_iT_s\mathbf{C}\hat{\mathbf{x}}(k)+\tilde{u}(k-1), \tag{11}$$

in (10) yields:

$$\begin{aligned}\bar{u}(k) &= -\left(K_p + K_i T_s\right)\mathbf{C}\hat{\mathbf{x}}(k) - \tilde{u}(k-1)\\ &= \left(K_p + K_i T_s\right)\mathbf{C}\mathbf{x}(k) - \left(K_p + K_i T_s\right)\mathbf{C}\mathbf{x}(k) - \left(K_p + K_i T_s\right)\mathbf{C}\hat{\mathbf{x}}(k) - \tilde{u}(k-1)\\ &= \left(K_p + K_i T_s\right)\mathbf{C}\left(\mathbf{x}(k) - \hat{\mathbf{x}}(k)\right) - \left(K_p + K_i T_s\right)\mathbf{C}\mathbf{x}(k) - \tilde{u}(k-1).\end{aligned} \tag{12}$$

Using (8) in (12) yields:

$$\bar{u}(k) = \left(K_p + K_i T_s\right)\mathbf{C}\mathbf{e}(k) - \left(K_p + K_i T_s\right)\mathbf{C}\mathbf{x}(k) - \tilde{u}(k-1). \tag{13}$$

Similarly, (11) can be represented using (8) as:

$$\begin{aligned}\tilde{u}(k) &= K_i T_s \mathbf{C}\sum_{i=1}^{k}\hat{\mathbf{x}}(i) = K_i T_s \mathbf{C}\hat{\mathbf{x}}(k) + \tilde{u}(k-1)\\ &= K_i T_s \mathbf{C}\mathbf{x}(k) - K_i T_s \mathbf{C}\mathbf{x}(k) + K_i T_s \mathbf{C}\hat{\mathbf{x}}(k) + \tilde{u}(k-1)\\ &= K_i T_s \mathbf{C}\mathbf{x}(k) - K_i T_s \mathbf{C}\left(\mathbf{x}(k) - \hat{\mathbf{x}}(k)\right) + \tilde{u}(k-1)\\ &= K_i T_s \mathbf{C}\mathbf{x}(k) - K_i T_s \mathbf{C}\mathbf{e}(k) + \tilde{u}(k-1).\end{aligned} \tag{14}$$

Now using (12) in (1) and using (8) yields:

$$\begin{aligned}\mathbf{x}(k+1) &= \mathbf{F}\mathbf{x}(k) + \mathbf{G}\bar{u}(k)\\ &= \mathbf{F}\mathbf{x}(k) + \mathbf{G}\left[-\left(K_p + K_i T_s\right)\mathbf{C}\hat{\mathbf{x}}(k) - \tilde{u}(k-1)\right]\\ &= \mathbf{F}\mathbf{x}(k) - \mathbf{G}\left(K_p + K_i T_s\right)\mathbf{C}\hat{\mathbf{x}}(k) - \mathbf{G}\tilde{u}(k-1)\\ &= \mathbf{F}\mathbf{x}(k) - \mathbf{G}\left(K_p + K_i T_s\right)\mathbf{C}\hat{\mathbf{x}}(k) - \mathbf{G}\tilde{u}(k-1) + \mathbf{G}\left(K_p + K_i T_s\right)\mathbf{C}\mathbf{x}(k) - \mathbf{G}\left(K_p + K_i T_s\right)\mathbf{C}\mathbf{x}(k)\\ &= \mathbf{F}\mathbf{x}(k) - \mathbf{G}\left(K_p + K_i T_s\right)\mathbf{C}\mathbf{x}(k) - \mathbf{G}\tilde{u}(k-1) + \mathbf{G}\left(K_p + K_i T_s\right)\mathbf{C}\left(\mathbf{x}(k) - \hat{\mathbf{x}}(k)\right)\\ &= \mathbf{F}\mathbf{x}(k) - \mathbf{G}\left(K_p + K_i T_s\right)\mathbf{C}\mathbf{x}(k) - \mathbf{G}\tilde{u}(k-1) + \mathbf{G}\left(K_p + K_i T_s\right)\mathbf{C}\mathbf{e}(k).\end{aligned} \tag{15}$$

Again,

$$\begin{aligned}\mathbf{e}(k+1) &= \mathbf{x}(k+1) - \hat{\mathbf{x}}(k+1)\\ &= \mathbf{F}\mathbf{x}(k) + \mathbf{G}\bar{u}(k) - \mathbf{F}\hat{\mathbf{x}}(k) - \mathbf{G}\bar{u}(k) - \mathbf{L}\left(\bar{y}(k) - \hat{y}(k)\right)\\ &= \mathbf{F}\left(\mathbf{x}(k) - \hat{\mathbf{x}}(k)\right) - \mathbf{L}\mathbf{C}\left(\mathbf{x}(k) - \hat{\mathbf{x}}(k)\right)\\ &= \left(\mathbf{F} - \mathbf{L}\mathbf{C}\right)\mathbf{e}(k).\end{aligned} \tag{16}$$

Now defining the augmented state vector as:

$$\mathbf{z}(k) = \left[\mathbf{x}^T(k) \quad \mathbf{e}^T(k) \quad \bar{u}^T(k-1) \quad \tilde{u}^T(k-1) \quad \bar{y}^T(k-1)\right]^T, \tag{17}$$

and using (7), (13)-(16), the NCS in (6) can be represented as:

$$\mathbf{z}(k+1) = \tilde{\mathbf{\Phi}}_1 \mathbf{z}(k) = \begin{bmatrix} \mathbf{F} - \mathbf{G}\mathbf{C}\left(K_p + K_i T_s\right) & \mathbf{G}\mathbf{C}\left(K_p + K_i T_s\right) & \mathbf{0} & -\mathbf{G} & \mathbf{0} \\ \mathbf{0} & \mathbf{F} - \mathbf{L}\mathbf{C} & \mathbf{0} & \mathbf{0} & \mathbf{0} \\ -\mathbf{C}\left(K_p + K_i T_s\right) & \mathbf{C}\left(K_p + K_i T_s\right) & \mathbf{0} & -\mathbf{I} & \mathbf{0} \\ \mathbf{C}K_i T_s & -\mathbf{C}K_i T_s & \mathbf{0} & \mathbf{I} & \mathbf{0} \\ \mathbf{C} & \mathbf{0} & \mathbf{0} & \mathbf{0} & \mathbf{0} \end{bmatrix} \mathbf{z}(k). \tag{18}$$

Case 2: Similarly, for the $\{\bar{s}_1, s_2\}$ condition i.e. packet drop in feedback path only we get:

$$\bar{y}(k) = \bar{y}(k-1), \tag{19}$$

and the terms $\bar{u}(k), \tilde{u}(k), \mathbf{x}(k+1)$ will remain same as in case 1 i.e. (13), (14), (15) respectively and the error term $\mathbf{e}(k+1)$ is:

$$\begin{aligned}\mathbf{e}(k+1) &= \mathbf{x}(k+1) - \hat{\mathbf{x}}(k+1)\\ &= \mathbf{F}\mathbf{x}(k) + \mathbf{G}\bar{u}(k) - \mathbf{F}\hat{\mathbf{x}}(k) - \mathbf{G}\bar{u}(k) - \mathbf{L}\left(\bar{y}(k-1) - \hat{y}(k)\right)\\ &= \mathbf{F}\left(\mathbf{x}(k) - \hat{\mathbf{x}}(k)\right) - \mathbf{L}\bar{y}(k-1) + \mathbf{L}\mathbf{C}\mathbf{x}(k) - \mathbf{L}\mathbf{C}\left(\mathbf{x}(k) - \hat{\mathbf{x}}(k)\right)\\ &= \left(\mathbf{F} - \mathbf{L}\mathbf{C}\right)\mathbf{e}(k) - \mathbf{L}\bar{y}(k-1) + \mathbf{L}\mathbf{C}\mathbf{x}(k).\end{aligned} \tag{20}$$

Using (13)-(15), (19)-(20) and considering augmented states as (17), the NCS can be represented as:

$$\mathbf{z}(k+1)=\tilde{\mathbf{\Phi}}_2\mathbf{z}(k)=\begin{bmatrix}\mathbf{F}-\mathbf{GC}\left(K_p+K_iT_s\right) & \mathbf{GC}\left(K_p+K_iT_s\right) & \mathbf{0} & -\mathbf{G} & \mathbf{0}\\ \mathbf{LC} & \mathbf{F}-\mathbf{LC} & \mathbf{0} & \mathbf{0} & -\mathbf{L}\\ -\mathbf{C}\left(K_p+K_iT_s\right) & \mathbf{C}\left(K_p+K_iT_s\right) & \mathbf{0} & -\mathbf{I} & \mathbf{0}\\ \mathbf{C}K_iT_s & -\mathbf{C}K_iT_s & \mathbf{0} & \mathbf{I} & \mathbf{0}\\ \mathbf{0} & \mathbf{0} & \mathbf{0} & \mathbf{0} & \mathbf{I}\end{bmatrix}\mathbf{z}(k). \tag{21}$$

Case 3: Similarly, for $\{s_1,\bar{s}_2\}$ i.e. packet drop occurring in the forward path only, then following conditions can be derived. The term $\bar{y}(k)$ and $\mathbf{e}(k+1)$ will remain same as case 1 i.e. (7) and (16) respectively and the following will hold:

$$\bar{u}(k)=\bar{u}(k-1), \tag{22}$$

$$\tilde{u}(k)=\tilde{u}(k-1), \tag{23}$$

$$\mathbf{x}(k+1)=\mathbf{F}\mathbf{x}(k)+\mathbf{G}\bar{u}(k-1). \tag{24}$$

Now using (7), (16)-(17), (22)-(24), the NCS (6) can be represented as:

$$\mathbf{z}(k+1)=\tilde{\mathbf{\Phi}}_3\mathbf{z}(k)=\begin{bmatrix}\mathbf{F} & \mathbf{0} & \mathbf{G} & \mathbf{0} & \mathbf{0}\\ \mathbf{0} & \mathbf{F}-\mathbf{LC} & \mathbf{0} & \mathbf{0} & \mathbf{0}\\ \mathbf{0} & \mathbf{0} & \mathbf{I} & \mathbf{0} & \mathbf{0}\\ \mathbf{0} & \mathbf{0} & \mathbf{0} & \mathbf{I} & \mathbf{0}\\ \mathbf{C} & \mathbf{0} & \mathbf{0} & \mathbf{0} & \mathbf{0}\end{bmatrix}\mathbf{z}(k). \tag{25}$$

Case 4: For $\{\bar{s}_1,\bar{s}_2\}$ i.e. packet drop occurring in both sides (feedback and forward path), the terms $\bar{y}(k),\bar{u}(k),\tilde{u}(k),\mathbf{x}(k+1)$ and $\mathbf{e}(k+1)$ will remain the same as (19), (22), (23), (24) and (20) respectively. Now using these equations, the NCS can be formulated as:

$$\mathbf{z}(k+1)=\tilde{\mathbf{\Phi}}_4\mathbf{z}(k)=\begin{bmatrix}\mathbf{F} & \mathbf{0} & \mathbf{G} & \mathbf{0} & \mathbf{0}\\ \mathbf{LC} & \mathbf{F}-\mathbf{LC} & \mathbf{0} & \mathbf{0} & -\mathbf{L}\\ \mathbf{0} & \mathbf{0} & \mathbf{I} & \mathbf{0} & \mathbf{0}\\ \mathbf{0} & \mathbf{0} & \mathbf{0} & \mathbf{I} & \mathbf{0}\\ \mathbf{0} & \mathbf{0} & \mathbf{0} & \mathbf{0} & \mathbf{I}\end{bmatrix}\mathbf{z}(k). \tag{26}$$

2.2 NCS with Observer based PID Controller

Here, the NCS has been modeled using discrete time plant and observer based PID controller. For this case, it is assumed that the last packet is effectively transmitted before the packet drop occurs.

Case 1: Under no-drop condition i.e. $\{s_1,s_2\}$ and with the assumption of reference inputs $R(k-1)=0$ and $R(k)=0$, the PID controller output using (4), (8), (11) and $\hat{y}(k)=\mathbf{C}\hat{\mathbf{x}}(k)$ is

$$\begin{aligned}
&\bar{u}(k)=u(k)\\
&=-K_p\hat{y}(k)-K_iT_s\sum_{i=1}^{k}\hat{y}(i)-\frac{K_d}{T_s}\left(\hat{y}(k)-\hat{y}(k-1)\right)\\
&=-\left(K_p+K_iT_s+\frac{K_d}{T_s}\right)\mathbf{C}\hat{\mathbf{x}}(k)-\tilde{u}(k-1)+\frac{K_d}{T_s}\mathbf{C}\hat{\mathbf{x}}(k-1)\\
&=\left(K_p+K_iT_s+\frac{K_d}{T_s}\right)\mathbf{C}\mathbf{x}(k)-\left(K_p+K_iT_s+\frac{K_d}{T_s}\right)\mathbf{C}\mathbf{x}(k)-\left(K_p+K_iT_s+\frac{K_d}{T_s}\right)\mathbf{C}\hat{\mathbf{x}}(k)-\tilde{u}(k-1)+\frac{K_d}{T_s}\mathbf{C}\hat{\mathbf{x}}(k-1)\quad+\frac{K_d}{T_s}\mathbf{C}\mathbf{x}(k-1)\\
&\quad-\frac{K_d}{T_s}\mathbf{C}\mathbf{x}(k-1)\\
&=-\left(K_p+K_iT_s+\frac{K_d}{T_s}\right)\mathbf{C}\mathbf{x}(k)+\left(K_p+K_iT_s+\frac{K_d}{T_s}\right)\mathbf{C}\mathbf{e}(k)-\tilde{u}(k-1)+\frac{K_d}{T_s}\mathbf{C}\mathbf{x}(k-1)-\frac{K_d}{T_s}\mathbf{C}\mathbf{e}(k-1).
\end{aligned} \tag{27}$$

Now using (27) in (1) and using (8) yields:

$$\begin{aligned}\mathbf{x}(k+1) &= \mathbf{F}\mathbf{x}(k)+\mathbf{G}\bar{u}(k)\\ &= \mathbf{F}\mathbf{x}(k)+\mathbf{G}\left[-\left(K_p+K_iT_s+\frac{K_d}{T_s}\right)\mathbf{C}\mathbf{x}(k)+\frac{K_d}{T_s}\mathbf{C}\mathbf{x}(k-1)+\left(K_p+K_iT_s+\frac{K_d}{T_s}\right)\mathbf{C}\mathbf{e}(k)-\frac{K_d}{T_s}\mathbf{C}\mathbf{e}(k-1)-\tilde{u}(k-1)\right].\end{aligned} \tag{28}$$

Similarly, from (1) the system can be written as:

$$\mathbf{x}(k)=\mathbf{F}\mathbf{x}(k-1)+\mathbf{G}\bar{u}(k-1). \tag{29}$$

Again from (16),

$$\mathbf{e}(k)=(\mathbf{F}-\mathbf{L}\mathbf{C})\mathbf{e}(k-1). \tag{30}$$

Now defining the new augmented state vector as:

$$\mathbf{z}(k)=\left[\mathbf{x}^T(k),\quad \mathbf{x}^T(k-1),\quad \mathbf{e}^T(k),\quad \mathbf{e}^T(k-1),\bar{u}^T(k-1),\quad \tilde{u}^T(k-1),\quad \bar{y}^T(k-1)\right]^T, \tag{31}$$

and representing:

$$\alpha=\left(K_p+K_iT_s+\frac{K_d}{T_s}\right), \tag{32}$$

and using (7), (14), (16), and (27)-(30), the NCS (6) can be formulated as:

$$\mathbf{z}(k+1)=\tilde{\mathbf{\Phi}}_1\mathbf{z}(k)=\begin{bmatrix}\mathbf{F}-\mathbf{G}\mathbf{C}\alpha & \mathbf{G}\mathbf{C}\frac{K_d}{T_s} & \mathbf{G}\mathbf{C}\alpha & -\mathbf{G}\mathbf{C}\frac{K_d}{T_s} & \mathbf{0} & -\mathbf{G} & \mathbf{0}\\ \mathbf{F} & \mathbf{0} & \mathbf{0} & \mathbf{0} & \mathbf{G} & \mathbf{0} & \mathbf{0}\\ \mathbf{0} & \mathbf{0} & \mathbf{F}-\mathbf{L}\mathbf{C} & \mathbf{0} & \mathbf{0} & \mathbf{0} & \mathbf{0}\\ \mathbf{0} & \mathbf{0} & \mathbf{0} & \mathbf{F}-\mathbf{L}\mathbf{C} & \mathbf{0} & \mathbf{0} & \mathbf{0}\\ -\mathbf{C}\alpha & \mathbf{C}\frac{K_d}{T_s} & \mathbf{C}\alpha & -\mathbf{C}\frac{K_d}{T_s} & \mathbf{0} & -\mathbf{I} & \mathbf{0}\\ \mathbf{C}K_iT_s & \mathbf{0} & -\mathbf{C}K_iT_s & \mathbf{0} & \mathbf{0} & \mathbf{I} & \mathbf{0}\\ \mathbf{C} & \mathbf{0} & \mathbf{0} & \mathbf{0} & \mathbf{0} & \mathbf{0} & \mathbf{0}\end{bmatrix}\mathbf{z}(k). \tag{33}$$

Case 2: For $\{\bar{s}_1, s_2\}$ condition i.e. packet drop in feedback path only we get:

$$\begin{aligned}\mathbf{e}(k) &= \mathbf{x}(k)-\hat{\mathbf{x}}(k)\\ &= \mathbf{F}\mathbf{x}(k-1)+\mathbf{G}\bar{u}(k-1)-\mathbf{F}\hat{\mathbf{x}}(k-1)-\mathbf{G}\bar{u}(k-1)-\mathbf{L}\left(\bar{y}(k-1)-\hat{y}(k-1)\right)\\ &= \mathbf{F}\left(\mathbf{x}(k-1)-\hat{\mathbf{x}}(k-1)\right)-\mathbf{L}\bar{y}(k-1)+\mathbf{L}\mathbf{C}\mathbf{x}(k-1)-\mathbf{L}\mathbf{C}\left(\mathbf{x}(k-1)-\hat{\mathbf{x}}(k-1)\right)\\ &= (\mathbf{F}-\mathbf{L}\mathbf{C})\mathbf{e}(k-1)-\mathbf{L}\bar{y}(k-1)+\mathbf{L}\mathbf{C}\mathbf{x}(k-1),\end{aligned} \tag{34}$$

and the terms $\bar{u}(k), \tilde{u}(k), \mathbf{x}(k+1)$ will remain same as in case 1 and the error term $\mathbf{e}(k+1)$ will be as (20).

Now using (19)-(20), (14), (27)-(29), (32) and (34) considering augmented states as (31), the NCS (6) can be represented as:

$$\mathbf{z}(k+1)=\tilde{\mathbf{\Phi}}_2\mathbf{z}(k)=\begin{bmatrix}\mathbf{F}-\mathbf{G}\mathbf{C}\alpha & \mathbf{G}\mathbf{C}\frac{K_d}{T_s} & \mathbf{G}\mathbf{C}\alpha & -\mathbf{G}\mathbf{C}\frac{K_d}{T_s} & \mathbf{0} & -\mathbf{G} & \mathbf{0}\\ \mathbf{F} & \mathbf{0} & \mathbf{0} & \mathbf{0} & \mathbf{G} & \mathbf{0} & \mathbf{0}\\ \mathbf{L}\mathbf{C} & \mathbf{0} & \mathbf{F}-\mathbf{L}\mathbf{C} & \mathbf{0} & \mathbf{0} & \mathbf{0} & -\mathbf{L}\\ \mathbf{0} & \mathbf{L}\mathbf{C} & \mathbf{0} & \mathbf{F}-\mathbf{L}\mathbf{C} & \mathbf{0} & \mathbf{0} & -\mathbf{L}\\ -\mathbf{C}\alpha & \mathbf{C}\frac{K_d}{T_s} & \mathbf{C}\alpha & -\mathbf{C}\frac{K_d}{T_s} & \mathbf{0} & -\mathbf{I} & \mathbf{0}\\ \mathbf{C}K_iT_s & \mathbf{0} & -\mathbf{C}K_iT_s & \mathbf{0} & \mathbf{0} & \mathbf{I} & \mathbf{0}\\ \mathbf{0} & \mathbf{0} & \mathbf{0} & \mathbf{0} & \mathbf{0} & \mathbf{0} & \mathbf{I}\end{bmatrix}\mathbf{z}(k). \tag{35}$$

Case 3: For $\{s_1, \bar{s}_2\}$ i.e. packet drop occurring in the forward path only, then using (22)-(24), (16), (7), (29)-(30) and (32) with the consideration of (31), the corresponding NCS can be represented as:

$$\mathbf{z}(k+1)=\tilde{\mathbf{\Phi}}_3\mathbf{z}(k)=\begin{bmatrix}\mathbf{F}&\mathbf{0}&\mathbf{0}&\mathbf{0}&\mathbf{G}&\mathbf{0}&\mathbf{0}\\ \mathbf{0}&\mathbf{F}&\mathbf{0}&\mathbf{0}&\mathbf{G}&\mathbf{0}&\mathbf{0}\\ \mathbf{0}&\mathbf{0}&\mathbf{F}-\mathbf{LC}&\mathbf{0}&\mathbf{0}&\mathbf{0}&\mathbf{0}\\ \mathbf{0}&\mathbf{0}&\mathbf{0}&\mathbf{F}-\mathbf{LC}&\mathbf{0}&\mathbf{0}&\mathbf{0}\\ \mathbf{0}&\mathbf{0}&\mathbf{0}&\mathbf{0}&\mathbf{I}&\mathbf{0}&\mathbf{0}\\ \mathbf{0}&\mathbf{0}&\mathbf{0}&\mathbf{0}&\mathbf{0}&\mathbf{I}&\mathbf{0}\\ \mathbf{C}&\mathbf{0}&\mathbf{0}&\mathbf{0}&\mathbf{0}&\mathbf{0}&\mathbf{0}\end{bmatrix}\mathbf{z}(k). \tag{36}$$

Case 4: For $\{\bar{s}_1,\bar{s}_2\}$ i.e. packet drops occurring on both sides (feedback and forward paths), using (19)-(20), (22)-(24), (29) and (34), the NCS can be formulated with (31) as:

$$\mathbf{z}(k+1)=\tilde{\mathbf{\Phi}}_4\mathbf{z}(k)=\begin{bmatrix}\mathbf{F}&\mathbf{0}&\mathbf{0}&\mathbf{0}&\mathbf{G}&\mathbf{0}&\mathbf{0}\\ \mathbf{0}&\mathbf{F}&\mathbf{0}&\mathbf{0}&\mathbf{G}&\mathbf{0}&\mathbf{0}\\ \mathbf{LC}&\mathbf{0}&\mathbf{F}-\mathbf{LC}&\mathbf{0}&\mathbf{0}&\mathbf{0}&-\mathbf{L}\\ \mathbf{0}&\mathbf{LC}&\mathbf{0}&\mathbf{F}-\mathbf{LC}&\mathbf{0}&\mathbf{0}&-\mathbf{L}\\ \mathbf{0}&\mathbf{0}&\mathbf{0}&\mathbf{0}&\mathbf{I}&\mathbf{0}&\mathbf{0}\\ \mathbf{0}&\mathbf{0}&\mathbf{0}&\mathbf{0}&\mathbf{0}&\mathbf{I}&\mathbf{0}\\ \mathbf{0}&\mathbf{0}&\mathbf{0}&\mathbf{0}&\mathbf{0}&\mathbf{0}&\mathbf{I}\end{bmatrix}\mathbf{z}(k). \tag{37}$$

3. Stability Analysis and Controller Design Methodology for NCS

3.1 Stability Analysis and LMI Formulation with CCL Algorithm

The transit of a packet $y(k)$ from the sensor to the actuator involves transmission across two switches S_1 and S_2 with varying rates of effective transmission. Since it is assumed that the fraction of effective packet transmission is r, the fraction of ineffective transmissions across any switch can at most be $(1-r)$. It is assumed that r_1 and r_2 is the effective transmission rate across the switches S_1 and S_2 respectively. If the packets are going through the same shared medium, the packet transmission rates in the forward and feedback path can be considered as the same. Further assuming $r_1=r_2=r$, the probabilities of an effective transmission R_1,R_2,R_3,R_4 from the sensor to the actuator can be computed for each of the following four cases as:

$$\begin{aligned}&s_1,s_2: R_1=r^2,\\ &\bar{s}_1,s_2: R_2=(1-r)r,\\ &s_1,\bar{s}_2: R_3=r(1-r),\\ &\bar{s}_1,\bar{s}_2: R_4=(1-r)(1-r).\end{aligned} \tag{38}$$

Then as reported and proved in [39], [43], [4] the NCS (6) is stable under packet-drop if the following inequality holds:

$$\beta_1^{R_1}\beta_2^{R_2}\beta_3^{R_3}\beta_4^{R_4}>\beta>1:\beta_1,\beta_2,\beta_3,\beta_4\in\mathbb{R}_+, \tag{39}$$

and the following Theorem 1 is satisfied.

***Theorem 1*:** The NCS (6) is exponentially stable with discrete time observer and PI/PID controller gains, for the subsystems $\tilde{\mathbf{\Phi}}_\sigma=f\{\mathbf{L},K_p,K_i,K_d\}$ and decay rate $\beta>0$ if there exists a common positive definite matrix $\mathbf{P}=\mathbf{P}^T>\mathbf{0}$ for which the following LMI is satisfied:

$$\begin{bmatrix}-\mathbf{P}&\beta_\sigma\tilde{\mathbf{\Phi}}_\sigma^T\\ \beta_\sigma\tilde{\mathbf{\Phi}}_\sigma&-\mathbf{Q}\end{bmatrix}<\mathbf{0}\quad\forall\sigma=1,2,3,4, \tag{40}$$

where, $\mathbf{P}^{-1}=\mathbf{Q}$ that implies

$$\mathbf{PQ}=\mathbf{I}. \tag{41}$$

Here, $\{\mathbf{P},\mathbf{Q}\}$ are the symmetric positive definite matrices of appropriate dimension.

***Proof*:** Defining Lyapunov function $V(\mathbf{z}(k))=\mathbf{z}^T(k)\mathbf{P}\mathbf{z}(k)$ the following inequality must hold for exponential stability:

$$V(\mathbf{z}(k+1))-V(\mathbf{z}(k))<(\beta_\sigma^{-2}-1)V(\mathbf{z}(k)). \tag{42}$$

Using (6) in (42) yields:

$$\tilde{\mathbf{\Phi}}_{\sigma}^{T}\mathbf{P}\tilde{\mathbf{\Phi}}_{\sigma}-\beta_{\sigma}^{-2}\mathbf{P}<\mathbf{0}, \tag{43}$$

which hold for each of the following sub-systems:

$$\begin{aligned}&\tilde{\mathbf{\Phi}}_{1}^{T}\mathbf{P}\tilde{\mathbf{\Phi}}_{1}-\beta_{1}^{-2}\mathbf{P}<\mathbf{0},\\&\tilde{\mathbf{\Phi}}_{2}^{T}\mathbf{P}\tilde{\mathbf{\Phi}}_{2}-\beta_{2}^{-2}\mathbf{P}<\mathbf{0},\\&\tilde{\mathbf{\Phi}}_{3}^{T}\mathbf{P}\tilde{\mathbf{\Phi}}_{3}-\beta_{3}^{-2}\mathbf{P}<\mathbf{0},\\&\tilde{\mathbf{\Phi}}_{4}^{T}\mathbf{P}\tilde{\mathbf{\Phi}}_{4}-\beta_{4}^{-2}\mathbf{P}<\mathbf{0}.\end{aligned} \tag{44}$$

Now, multiplying both side of (43) by β_{σ}^{2} and taking Schur complement yields (40) with the assumption $\mathbf{P}^{-1}=\mathbf{Q}$. □

However, it can be seen that Theorem 1 is not representing the strict LMI condition due to the presence of (41). This type of non-convex feasibility problem can be overcome by converting it into a sequential optimization problem subjected to LMI constraints using the CCL algorithm proposed in [37] and has been used here. As per the CCL algorithm if the LMI $\begin{bmatrix}\mathbf{P}&\mathbf{I}\\\mathbf{I}&\mathbf{Q}\end{bmatrix}\geq\mathbf{0}$ is feasible in the matrix variables $\mathbf{P}\in\mathbb{R}^{n}>\mathbf{0}$ and $\mathbf{Q}\in\mathbb{R}^{n}>\mathbf{0}$, then $\mathrm{Tr}(\mathbf{PQ})\geq n$, and at the optimum $\mathrm{Tr}(\mathbf{PQ})=n$ iff $\mathbf{PQ}=\mathbf{I}$. In [50], the CCL algorithm has been used to solve LMIs with a nonconvex constraints to solve H_{∞} model reduction problem of Markovian jump linear systems. In [51], the CCL algorithm has been used to formulate the nonconvex feasibility problem into a sequential minimization problem subjected to LMI constraints that are established by defining H_{∞} performance criterion in order to solve H_{∞} controller design problems. In [52], the stability conditions of NCS considering random time delay and arbitrary packet dropout are derived as LMIs with strict and nonconvex constraints and are solved by converting them into a sequential optimization problem using the CCL algorithm. In [53], a state feedback controller with certain H_{∞} disturbance level has been designed for NCS considering both network induced delays and packet dropouts by solving LMIs with nonconvex constraints using CCL. It is important to note that the sub-systems (6) are functions of observer and PI/PID controller gains i.e. $\tilde{\mathbf{\Phi}}_{\sigma}=f\{\mathbf{L},K_{p},K_{i},K_{d}\}$. Therefore, representing (41) in an LMI form yields:

$$\begin{bmatrix}\mathbf{P}&\mathbf{I}\\\mathbf{I}&\mathbf{Q}\end{bmatrix}\geq\mathbf{0}, \tag{45}$$

and using the CCL algorithm, the observer and PI/PID controller gains can be obtained by solving the following minimization problem with LMI constraints:

$$\min\mathrm{Tr}(\mathbf{PQ}), \tag{46}$$

subjected to (39), (40) and (45).

3.2 Iterative Joint Observer and Controller Design Algorithm

The main objective of this paper is to find a joint set of observer and PI/PID controller gains to achieve satisfactory closed loop performance while guaranteeing exponential stability of the NCS (6) under random packet dropout. In order to achieve this, the following steps are to be followed [37]:

***Step 1*:** Initialize values of r and $\beta_{i}, i\in 1,2,3,4$ subject to (38) and (39).

***Step 2*:** Set the default values of sdpsettings as solver = 'sedumi', sedumi.eps = 10^{-12}.

***Step 3*:** Find a feasible solution set $\{\mathbf{P}(k),\mathbf{Q}(k),\mathbf{L}(k),K_{p}(k),K_{i}(k),K_{d}(k)\}$ satisfying (40), (45) at $k=0$.

***Step 4*:** Set $k=k+1$ and solve the LMIs (40), (45) with the following constraints:

$$\min\mathrm{Tr}(\mathbf{PQ}(k)+\mathbf{P}(k)\mathbf{Q}). \tag{47}$$

***Step 5*:** Calculate the error:

$$\mathrm{err}=\mathrm{Tr}(\mathbf{PQ}(k)+\mathbf{P}(k)\mathbf{Q})-2\times\mathrm{size}(\mathbf{PQ},1); \tag{48}$$

elseif $\mathrm{err}\approx 0$, stop the loop and obtain the output $\{\mathbf{P},\mathbf{Q},\mathbf{L},K_{p},K_{i},K_{d}\}$;

else if $k>N$, where N is the maximum number of iterations allowed, stop the loop and obtain the output $\{\mathbf{P},\mathbf{Q},\mathbf{L},K_{p},K_{i},K_{d}\}$;

Otherwise go to Step 4.

***Step 6*:** Exit if the final output $\{\mathbf{P},\mathbf{Q},\mathbf{L},K_{p},K_{i},K_{d}\}$ satisfies (44).

In this paper, all the computations for the above algorithm are performed using the YALMIP Toolbox [54] in MATLAB by interfacing the external semi-definite optimization solver SeDuMi [55]. In order to obtain the variables $\{\mathbf{P},\mathbf{Q},\mathbf{L},K_{p},K_{i},K_{d}\}$ satisfying (40), (45) and (46), we have considered the number of iterations as $N=50$ for the above algorithm which is sufficient for the convergence of the CCL algorithm. The corresponding CCL error (i.e. err) in (48) has been shown in Figure 2 for two test-bench energy systems using observer based PI and PID controllers.

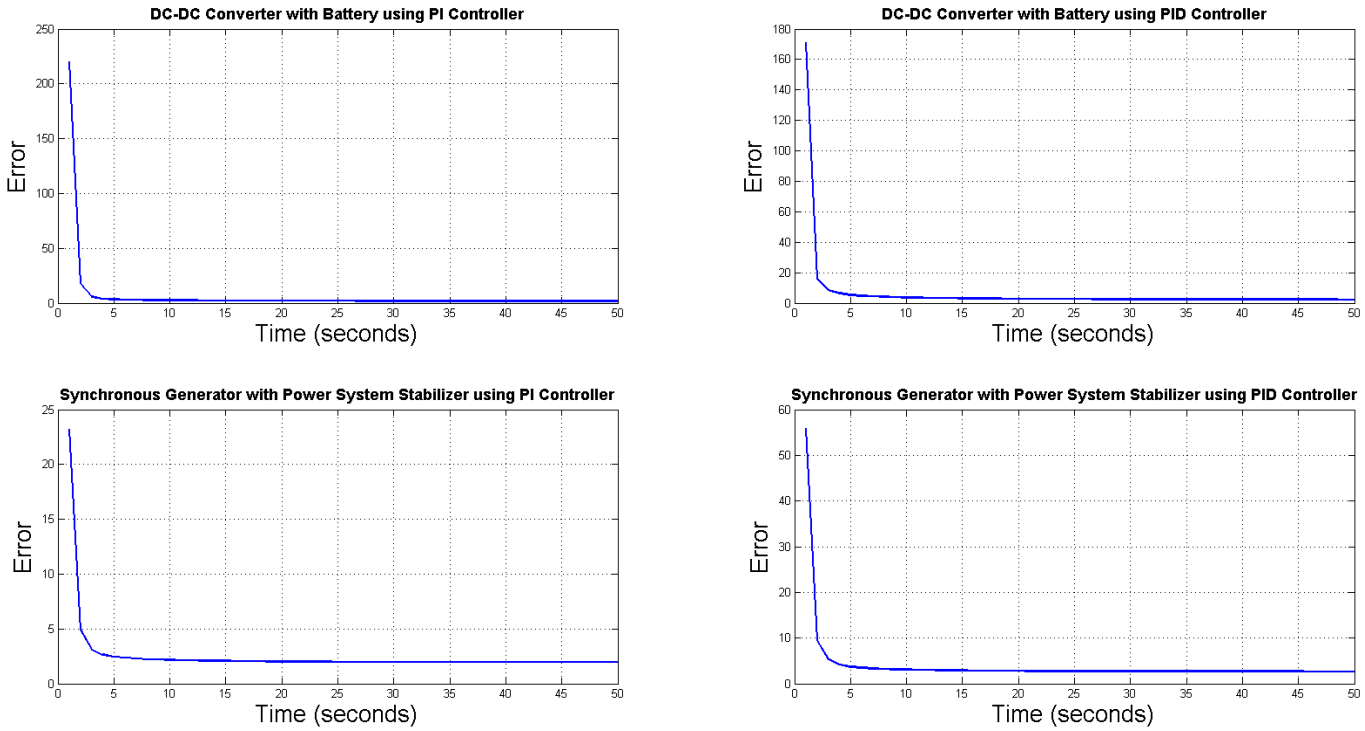

Figure 2: Convergence of error in the CCL algorithm for the two test-bench energy systems with observer-based PI/PID controller for specified 90% rate of packet drop.

4. Simulation Results for Test-Bench Plants

In this section, we have validated the proposed algorithm for two test bench systems i.e. battery with DC/DC converter and synchronous generator with power system stabilizer (PSS). In both the cases, these continuous time systems are discretized with the specified sampling time $T_s = 0.1\text{s}$.

4.1 Battery with DC/DC Converter

Here, model of a battery with DC/DC converter as in [56] has been used as a test energy system which can be represented as shown in Figure 3. The continuous time state space model for this system can be written as:

$$\dot{\mathbf{x}} = \mathbf{A}\mathbf{x} + \mathbf{B}u, \quad y = \mathbf{C}\mathbf{x}, \tag{49}$$

where, $\mathbf{x} = \begin{bmatrix} v_{Cb} & v_{Cs} & v_{\text{batt}} & i_{\text{batt}} \end{bmatrix}^T$ and $y = \begin{bmatrix} v_{Cb} & v_{Cs} & v_{\text{batt}} & i_{\text{batt}} \end{bmatrix}^T$ and $u = m_{\text{batt}}$. The system matrices are:

$$\mathbf{A} = \begin{bmatrix} a_{11} & a_{12} & 0 & b_{11} \\ a_{21} & a_{22} & 0 & b_{21} \\ a_{31} & 0 & a_{33} & b_{31} \\ 0 & 0 & \dfrac{1}{L_b} & -\dfrac{R_b}{L_b} \end{bmatrix}, \quad \mathbf{B} = \begin{bmatrix} 0 & 0 & 0 & -\dfrac{V_{\text{bus}}}{L_b} \end{bmatrix}^T, \quad \mathbf{C} = \begin{bmatrix} 0 & 0 & 0 & 1 \end{bmatrix}, \tag{50}$$

where, the constants of the system matrices are given by:

$$\begin{aligned} a_{11} &= \frac{-1}{C_{\text{bulk}}\left(R_e + R_{\text{surf}}\right)}, \; a_{12} = \frac{1}{C_{\text{bulk}}\left(R_e + R_{\text{surf}}\right)}, a_{31} = \frac{R_e + R_{\text{surf}}}{C_{\text{surf}}\left(R_e + R_{\text{surf}}\right)^2} - \frac{R_{\text{surf}}R_e + R_{\text{surf}}^2}{C_{\text{bulk}}R_e\left(R_e + R_{\text{surf}}\right)^2}, \\ a_{21} &= \frac{1}{C_{\text{surf}}\left(R_e + R_{\text{surf}}\right)}, \; a_{22} = \frac{-1}{C_{\text{surf}}\left(R_e + R_{\text{surf}}\right)}, a_{33} = \frac{R_{surf}}{R_e C_{\text{bulk}}\left(R_e + R_{\text{surf}}\right)} - \frac{1}{C_{\text{surf}}\left(R_e + R_{\text{surf}}\right)}, \\ b_{11} &= \frac{-R_{\text{surf}}}{C_{\text{bulk}}\left(R_e + R_{\text{surf}}\right)}, \; b_{21} = \frac{-R_e}{C_{\text{surf}}\left(R_e + R_{\text{surf}}\right)}, b_{31} = \frac{R_t R_{surf}}{C_{\text{bulk}}R_e\left(R_e + R_{\text{surf}}\right)} - \frac{R_t}{C_{\text{surf}}\left(R_e + R_{\text{surf}}\right)} - \frac{R_e R_{\text{surf}} + R_e^2}{C_{\text{surf}}\left(R_e + R_{\text{surf}}\right)^2}. \end{aligned} \tag{51}$$

Here, the state variables are bulk voltage, surface voltage, current coming out from the battery and output voltage of the battery. The variable descriptions and values are considered as: C_{bulk} = bulk capacitance of the battery = 29458 F, R_e = bulk resistance of the battery = 11.3 mΩ, C_{surf} = surface capacitance of the battery = 27.37 F, L_b = converter inductance = 0.56 mH, R_b =

converter resistance = 0.1 Ω, R_s = surface resistance of the battery = 11.3 mΩ, V_b = battery voltage = 6 V, R_t = terminal resistance of the battery = 8.2 mΩ. While incorporating more renewable energies in the power grids and electric vehicles in the transportation system, it is important to take efficient energy management decision based on the state of charge (SoC) and state of health (SoH) of the battery. Failure to measure the status of the battery can cause overcharging and over-discharging situations which can cause the decrease in the lifetime and efficiency of the battery pack. The parameters SoH and SoC is dependent upon the surface and bulk voltage of the battery [57].

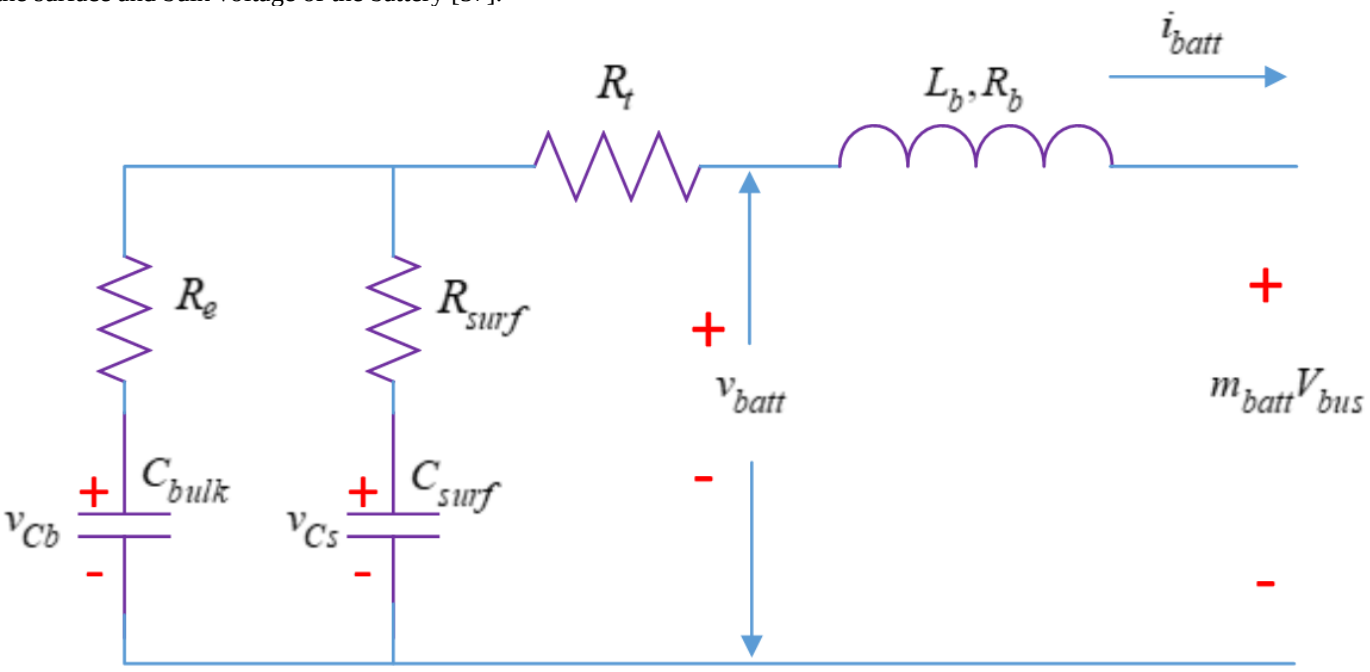

Figure 3: Schematic diagram of a DC/DC converter with battery.

Table 1: Observer gains obtained from the iterative LMI solver for the two test-bench plants

Energy System	**Observer Gain**	
	L_{PI}	**L_{PID}**
Battery and DC/DC Converter	[0.0116, 0.0103, 0.0097, 0.1662]^T	[0.0140, 0.0125, 0.0113, 0.1572]^T
Synchronous Generator	[-0.1218, 0.3178, -4.4631, -1.8597, -1.1749, -1.4395]^T	[-0.1917, 0.4924, -7.1376, -2.9504, -1.8614, -2.3289]^T

Table 2: PI/PID controller gains obtained from the LMI solver for the two test-bench plants

Energy System	**PI Controller**		**PID Controller**		
	K_p	K_i	K_p	K_i	K_d
Battery and DC/DC Converter	-0.004	-0.0061	-7.36×10^{-4}	-0.0066	3.62×10^{-7}
Synchronous Generator	1.8267	1.02×10^{-7}	1.1133	2.93×10^{-6}	-0.1304

Using the proposed algorithm for two test energy systems, the observer gains are calculated in Table 1 and PI/PID controller gains $\{\mathbf{L}, K_p, K_i, K_d\}$ are given in Table 2. These gains are obtained by considering the QoS or the rate of effective transmissions as $r_1 = r_2 = 0.1$ and choosing the smallest value of scalars $\beta_i, i \in 1,2,3,4$ as $\beta_1 = 1.1$, $\beta_2 = 0.65$, $\beta_3 = 0.65$, $\beta_4 = 1.1$ [9], [58] for the battery system. In the both feedback and forward paths, the output $\bar{y}(k)$ and the control input $\bar{u}(k)$ will be replaced by their previous instant's data i.e. $\bar{y}(k) = \bar{y}(k-1)$ and $\bar{u}(k) = \bar{u}(k-1)$ which are assumed to be updated by the last effective transmission's data. Since, this work considers an ADS approach for NCS, the data will be effectively transmitted with certain rate constraint *r* while ineffective transmission rate will be (1-*r*) across the network. Therefore, the present work aims a joint design of the observer and PI/PID controller with *r* = 0.1 i.e. 10% effective transmissions which means (1-*r*) = 0.9 i.e. higher (90%) ineffective transmissions rate across the communication network (represented by switch S_1 and S_2) of the NCS. The tuned controller and observer gains are then validated for both lower (50%) and higher (90%) rate of packet drops for the two test bench plants with higher order dynamics.

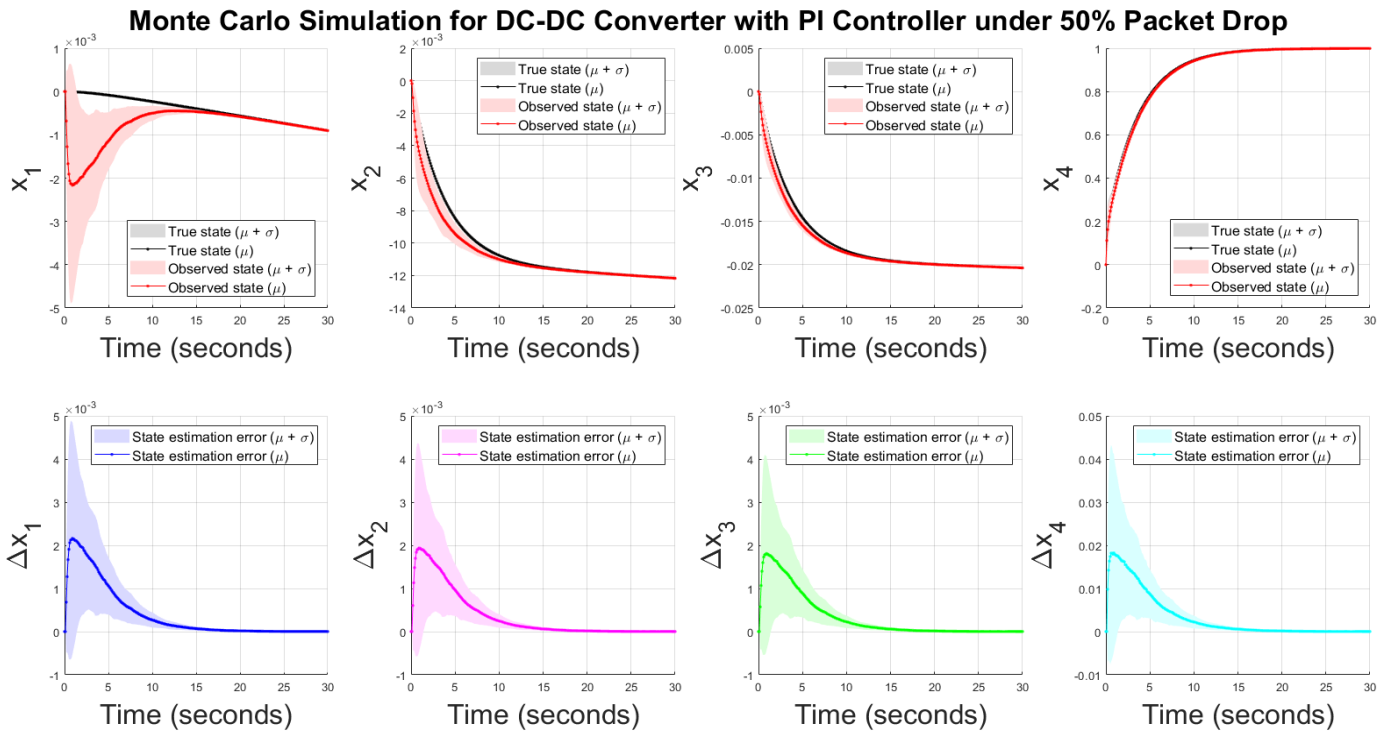

Figure 4: True/observed states and state estimation error using observer-based PI controller with 50% packet drop for discretized model of DC-DC converter with battery.

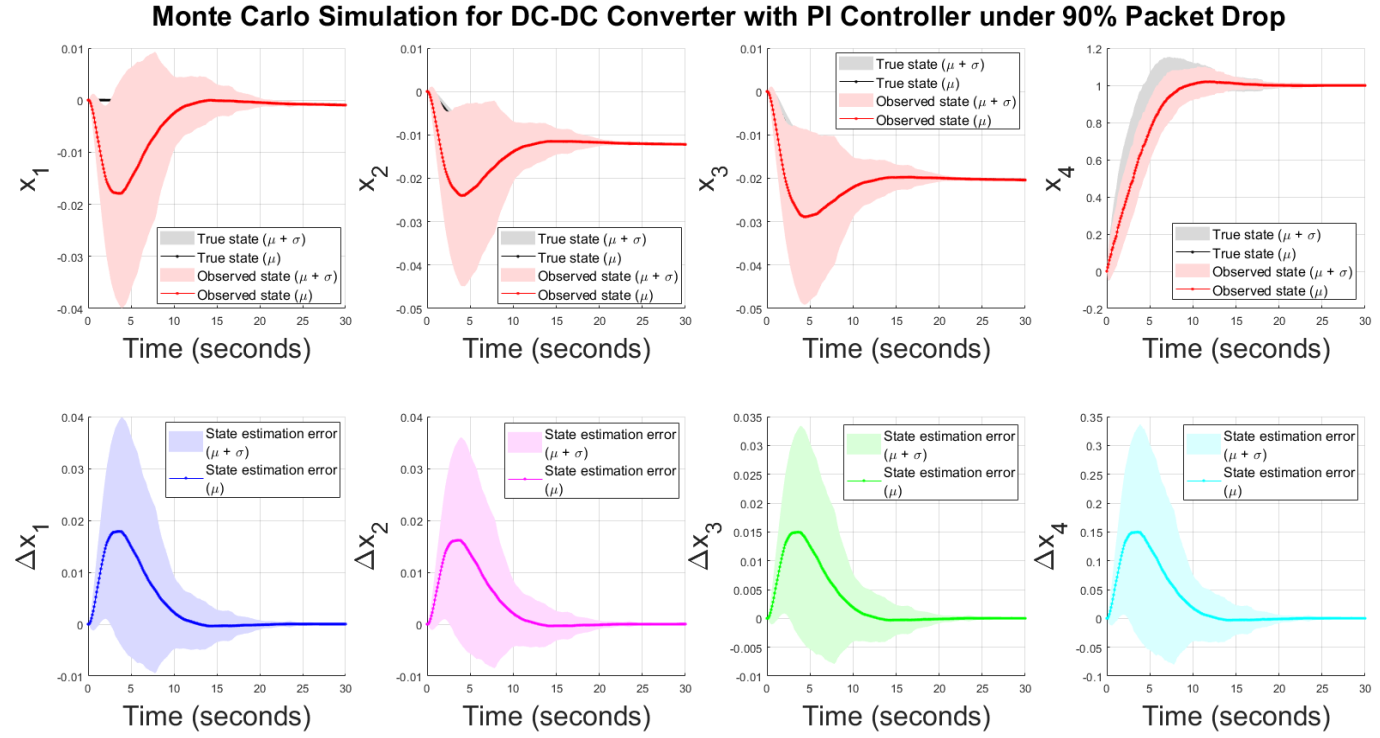

Figure 5: True/observed states and state estimation error using observer-based PI controller with 90% packet drop for discretized model of DC-DC converter with battery.

The average execution time for each iteration up to $N = 50$ for PI and PID controller for the battery with DC/DC converter is 0.5092(±0.0576) sec and 1.6266(±0.0872) sec, respectively. Therefore, the total computing time for the CCL algorithm to stabilize the DC-DC converter system with battery is 0.4243 min and 1.3555 min with the PI and PID controllers, respectively. In Table 1, the gains ($\mathbf{L}_{\mathrm{PI}}$) and ($\mathbf{L}_{\mathrm{PID}}$) represents the observer gains ($\mathbf{L}$) corresponding to PI/PID controller, respectively. Since packet loss is a random phenomenon although the controller design is deterministic, ensembles of random packet drops are

shown using 1000 Monte Carlo runs and the mean (μ) and standard deviations (std - σ) of the original, observed states and the state estimation errors at each time instant are shown in Figure 4 for medium packet drop rate (50%) and in Figure 5 for high probability of packet loss (90%) using the PI controllers with observers respectively. It is evident that the system settles within 30 sec, although the std of the estimation error is higher for the 90% packet drop case. In the bottom rows of all the time responses, we show the state estimation error for individual state variables i.e. the difference between the true and observed states represented by $\Delta \mathbf{x}_i, i \in \mathbb{Z}_+$.

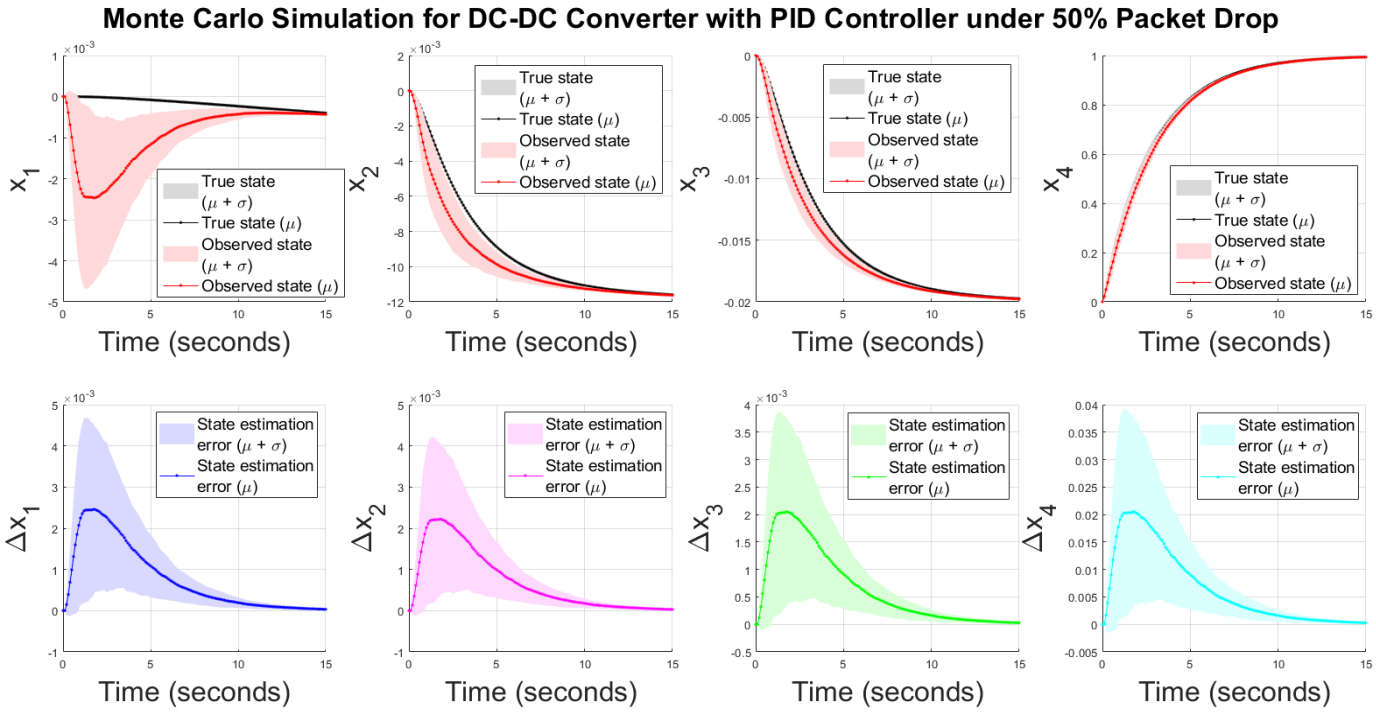

Figure 6: True/observed states and state estimation error using observer-based PID controller with 50% packet drop for discretized model of DC-DC converter with battery.

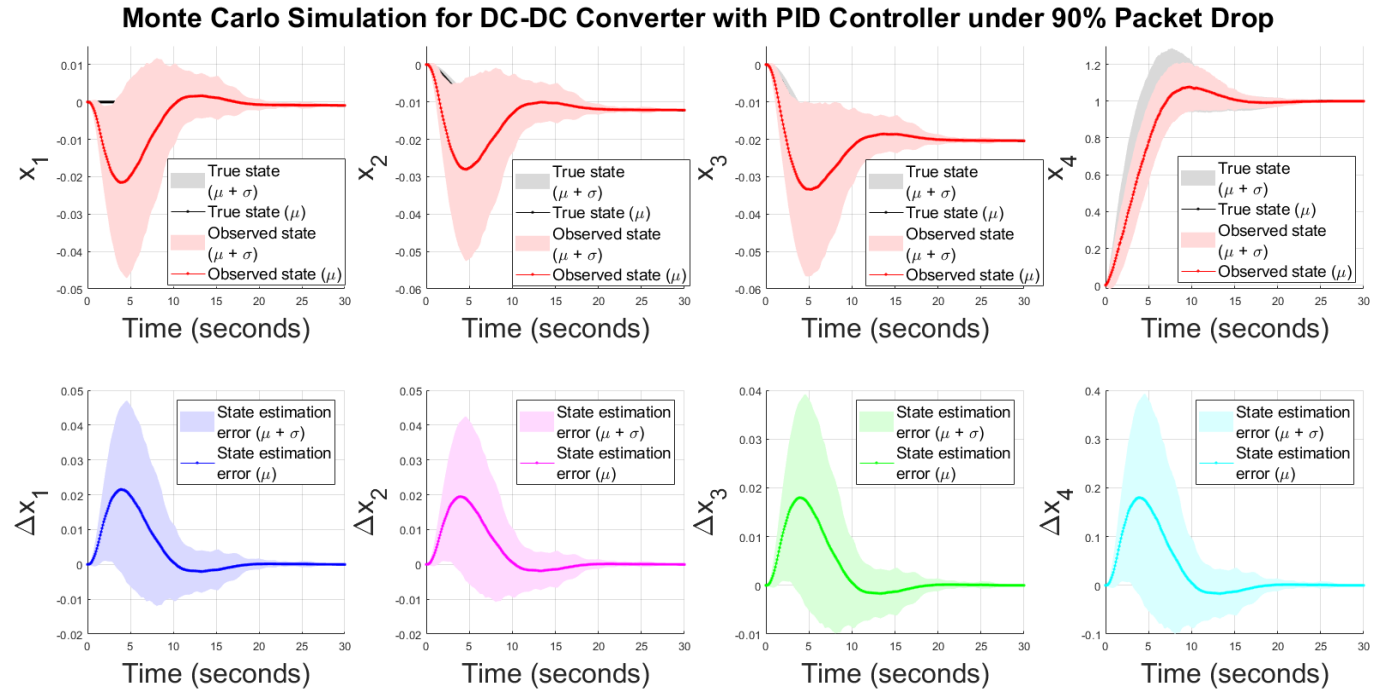

Figure 7: True/observed states and state estimation error using observer-based PID controller with 90% packet drop for discretized model of DC-DC converter with battery.

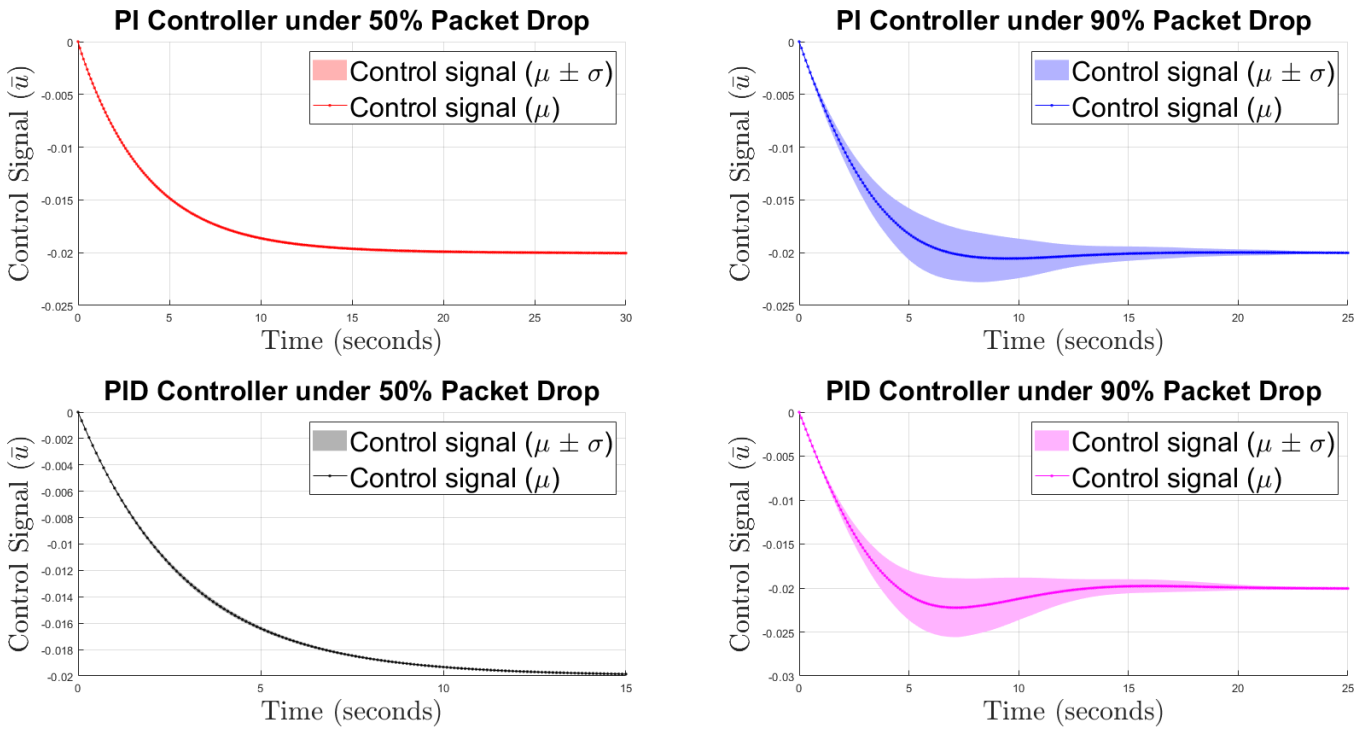

Figure 8: Control signal using observer-based PI and PID controller under 50% and 90% packet drop for discretized model of DC-DC converter with battery.

The true/estimated state trajectories and state estimation errors of DC/DC converter and battery are compared for 50% (Figure 6) and 90% (Figure 7) random packet drops in both sides of the control loop i.e. feedback and forward with the obtained observer gains and PID controller gains $\{\mathbf{L}, K_p, K_i, K_d\}$. It is evident that the designed controller can stabilize the system and yields satisfactory control performance under 50% packet drop rate. However, for 90% packet drop case, the oscillation in the states and estimation errors are slightly higher for the PID controller (Figure 7) as compared to the PI controller (Figure 5). This may be due to the fact that stochastic fluctuations under high rate of packet drops get amplified with the derivative action in the PID controller whereas PI controller yields a smoother response. Our simulation results show the error plots between the true and observed state variables indicating the efficacy of the observer in forcing the estimation error to converge quickly even in the presence of moderate to high rate of packet loss. Therefore, in this test-bench energy system application with NCS, a less complex controller with lesser degrees of freedom (DOF) i.e. PI controller is better suited than more complex one with higher DOF i.e. PID controller which may otherwise seem as counter-intuitive with respect to the previous findings in Pan *et al.* [30] where it was shown controllers with higher DOF may perform better in NCS applications. The corresponding control signal or manipulated variables to the system are shown in Figure 8 under 50% and 90% random packet loss using both PI and PID controllers respectively. It is evident that the control signal fluctuates more under 90% random packet loss case and with PID controller having higher std of the oscillations i.e. a higher control effort is required to handle such larger packet drop case.

4.2 Synchronous Generator with Power System Stabilizer

Online parameter estimation of the synchronous generator is important in the case of stability studies where system response has to be measured based on large disturbances. It is difficult to measure the change in synchronous generator angle which is a key component of power system stability studies. Hence an observer is required for the measurement of the generator angle from the other directly measurable states. Transient stability is defined as the ability of the generator system to recover from a large disturbance and given by the following state space model [59]:

$$\begin{bmatrix} \Delta\dot{\omega}_r \\ \Delta\dot{\delta} \\ \Delta\dot{\psi}_{fd} \\ \Delta\dot{v}_1 \\ \Delta\dot{v}_2 \\ \Delta\dot{v}_s \end{bmatrix} = \begin{bmatrix} a_{11} & a_{12} & a_{13} & 0 & 0 & 0 \\ a_{21} & 0 & 0 & 0 & 0 & 0 \\ 0 & a_{32} & a_{33} & a_{34} & 0 & a_{36} \\ 0 & a_{42} & a_{43} & a_{44} & 0 & 0 \\ a_{51} & a_{52} & a_{53} & 0 & a_{55} & 0 \\ a_{61} & a_{62} & a_{63} & 0 & a_{65} & a_{66} \end{bmatrix} \begin{bmatrix} \Delta\omega_r \\ \Delta\delta \\ \Delta\psi_{fd} \\ \Delta v_1 \\ \Delta v_2 \\ \Delta v_s \end{bmatrix} + \begin{bmatrix} b_{11} \\ 0 \\ 0 \\ 0 \\ b_{15} \\ b_{16} \end{bmatrix} \Delta T_m. \tag{52}$$

Here, the state variables can be represented as $\mathbf{x}=\left[\Delta\omega_r \quad \Delta\delta \quad \Delta\psi_{fd} \quad \Delta v_1 \quad \Delta v_2 \quad \Delta v_s\right]^T$ in the continuous time state space form (49) where, $\Delta\omega_r$ = change in angular speed of the rotor, $\Delta\delta$ = change in rotor angle, $\Delta\psi_{fd}$ = change in flux linkage with the field circuit in *d*-axis, Δv_1 = output after the terminal voltage is measured by voltage transducer, Δv_2 = speed the measured after the measured signal is passed through a high pass washout filter, Δv_s = the speed measured after there is a phase compensation between the measured signal and the field voltage. The control signal is $u=\Delta T_m$ and the output matrix is $C=\left[1 \quad 0 \quad 0 \quad 0 \quad 0 \quad 0\right]$. The constants of the system matrices are given as:

$$a_{11}=-\frac{K_D}{2H},\ a_{12}=-\frac{K_1}{2H},\ a_{13}=-\frac{K_2}{2H},\ a_{21}=\omega_0=2\pi f_0,\ a_{32}=-\frac{\omega_0 R_{fd}}{L_{fd}}m_1 L'_{ads},\ a_{33}=-\frac{\omega_0 R_{fd}}{L_{fd}}\left[1-\frac{L'_{ads}}{L_{fd}}+m_2 L'_{ads}\right],$$

$$b_{11}=\frac{1}{2H},\ b_{11}=\frac{\omega_0 R_{fd}}{L_{adu}},\ b_{32}=\frac{\omega_0 R_{fd}}{L_{adu}},\ a_{34}=-\frac{\omega_0 R_{fd}}{L_{adu}}K_A,\ a_{42}=\frac{K_5}{T_R},\ a_{43}=\frac{K_6}{T_R},\ a_{44}=-\frac{1}{T_R},\ a_{51}=K_{\mathrm{STAB}}a_{11},$$

$$a_{52}=K_{\mathrm{STAB}}a_{12},\ a_{53}=K_{\mathrm{STAB}}a_{13},\ a_{55}=-\frac{1}{T_W},\ a_{61}=\frac{T_1}{T_2}a_{51},$$

$$a_{62}=\frac{T_1}{T_2}a_{52},\ a_{63}=\frac{T_1}{T_2}a_{53},\ a_{66}=-\frac{1}{T_2},\ a_{61}=\frac{T_1}{T_2}a_{55}+\frac{1}{T_2},\ a_{36}=\frac{\omega_0 R_{fd}}{L_{adu}}K_A,\ b_{11}=\frac{1}{2H},\ b_{15}=\frac{K_{STAB}}{2H},\ b_{16}=\frac{T_1}{T_2}\frac{K_{STAB}}{2H},$$

$$m_1=\frac{E_B\left(X_{Tq}\sin\delta_0-R_{\mathrm{Td}}\cos\delta_0\right)}{D},\ n_1=\frac{E_B\left(R_T\sin\delta_0-X_{\mathrm{Td}}\cos\delta_0\right)}{D},\ m_2=\frac{X_{Tq}}{D}\frac{L_{ads}}{L_{ads}+L_{fd}},\ n_2=\frac{R_T}{D}\frac{L_{ads}}{L_{ads}+L_{fd}},\ L'_{ads}=\frac{1}{\frac{1}{L_{ads}}+\frac{1}{L_{fd}}},$$

$$K_1=n_1\left(\psi_{ad0}+L_{aqs}i_{d0}\right)-m_1\left(\psi_{aq0}+L'_{ads}i_{q0}\right),\ K_2=n_2\left(\psi_{ad0}+L_{aqs}i_{d0}\right)-m_2\left(\psi_{aq0}+L'_{ads}i_{q0}\right)+\frac{L'_{ads}}{L_{fd}}i_{q0},$$

$$K_5=\frac{e_{d0}}{E_{t0}}\left[-R_a m_1+L_l n_1+L_{aqs}n_1\right]+\frac{e_{q0}}{E_{t0}}\left[-R_a n_1+L_l m_1+L'_{ads}m_1\right],$$

$$K_6=\frac{e_{d0}}{E_{t0}}\left[-R_a m_2+L_l n_2+L_{aqs}n_2\right]+\frac{e_{q0}}{E_{t0}}\left[-R_a n_2+L_l m_2+L'_{ads}\left(\frac{1}{L_{fd}}-m_2\right)\right]. \tag{53}$$

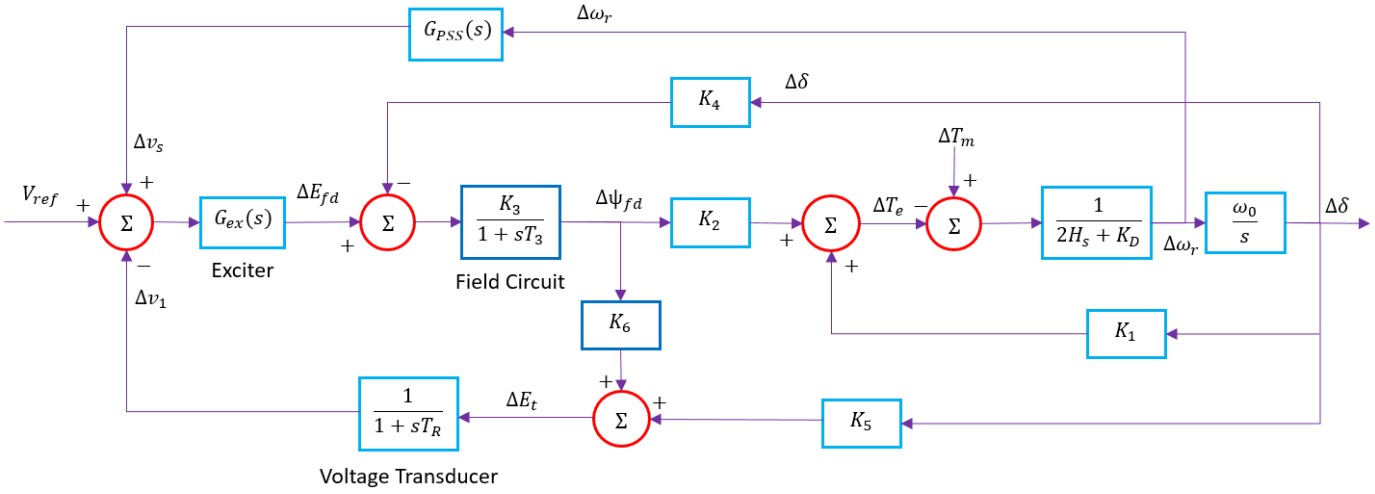

Figure 9: Schematic diagram of a synchronous generator with PSS.

The system constants are given as: K_D = damping torque coefficient in pu torque/pu speed deviation = 1000, H = inertia constant in MWs/MVA = 3.5, ω_0 = rated speed in electrical-rad/s = $2\pi f_0$ = 377 for a 60 Hz system, R_{fd} = rotor circuit resistance = 0.0006 Ohm, L_{fd} = rotor circuit inductance = 0.153 H, L_{ads} = mutual inductance between rotor and stator = 1.65 H, K_{STAB} = signal gain for the measured speed signal = 9.5, T_1, T_2 = time constants for the phase compensating filter = 0.154, 0.033, T_W = washout filter time constant = 1.4 sec, K_A = exciter gain = 200, T_R = time constant of the voltage transducer = 0.02

sec, L_{adu} = stator inductance = 1.65 H. The synchronous generator model with PSS can be represented in terms of a block diagram shown in Figure 9.

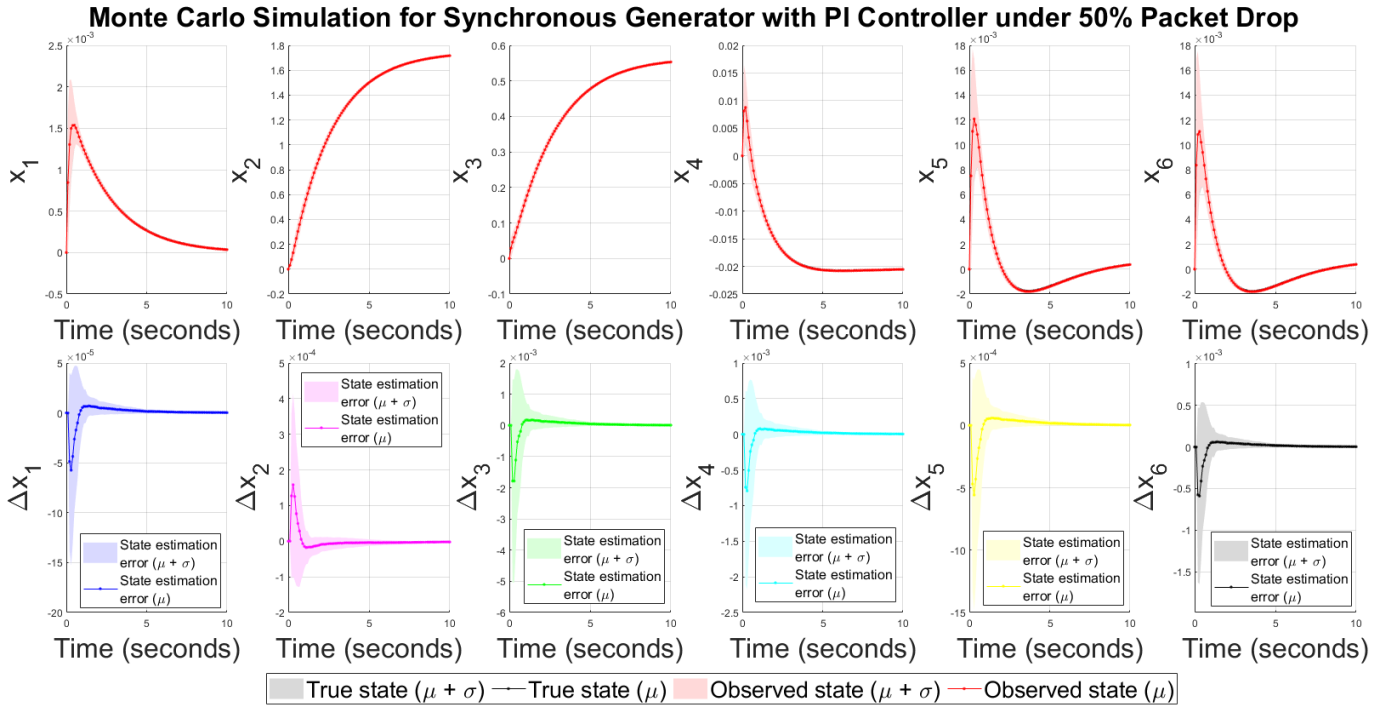

Figure 10: True/observed states and state estimation error using observer-based PI controller with 50% packet drop for the discretized model of synchronous generator with PSS. States $\mathbf{x}_1$ is converging to zero since the model is designed with equilibrium point zero because these are perturbation model.

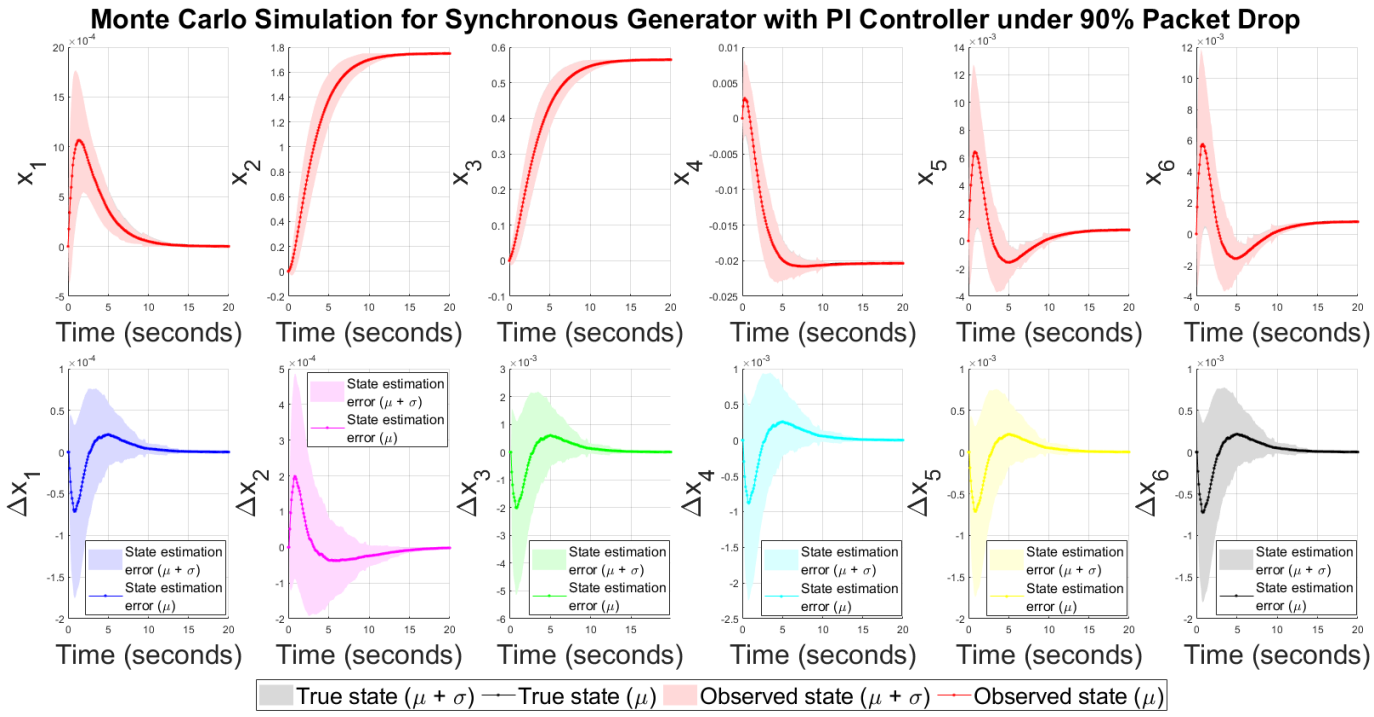

Figure 11: True/observed states and state estimation error using observer-based PI controller with 90% packet drop for the discretized model of synchronous generator with PSS.

Similar to previous test-bench energy system, here we have considered the QoS or the effective transmission rate as $r_1 = r_2 = 0.1$ and the other scalars are chosen as $\beta_1 = 1.1$, $\beta_2 = 0.65$, $\beta_3 = 0.65$, $\beta_4 = 1.1$ and the corresponding observer and

PI/PID controller gains are shown in Table 1-Table 2. The CCL convergence error have been shown in Figure 2 for obtaining the observer and PI/PID controller gains. The average computation time for 50 iterations for observer-based PI and PID controller for this synchronous generation with PSS system is 0.6058(±0.0481) sec and 3.7401(±0.1649) sec, respectively. Therefore, the total computing time for the CCL algorithm to stabilize the synchronous generator system with PSS is 0.5048 min and 3.1167 min with the PI and PID controllers, respectively.

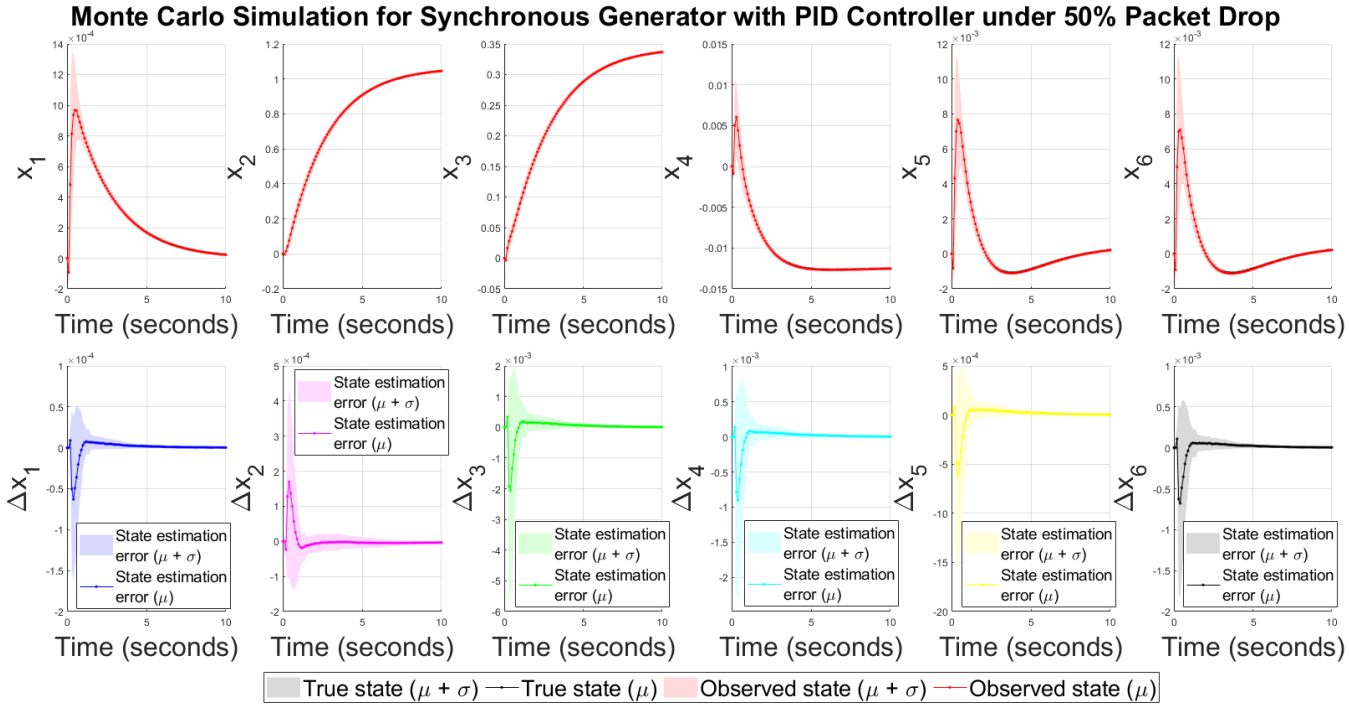

Figure 12: True/observed states and state estimation error using observer-based PID controller with 50% packet drop for the discretized model of synchronous generator with PSS.

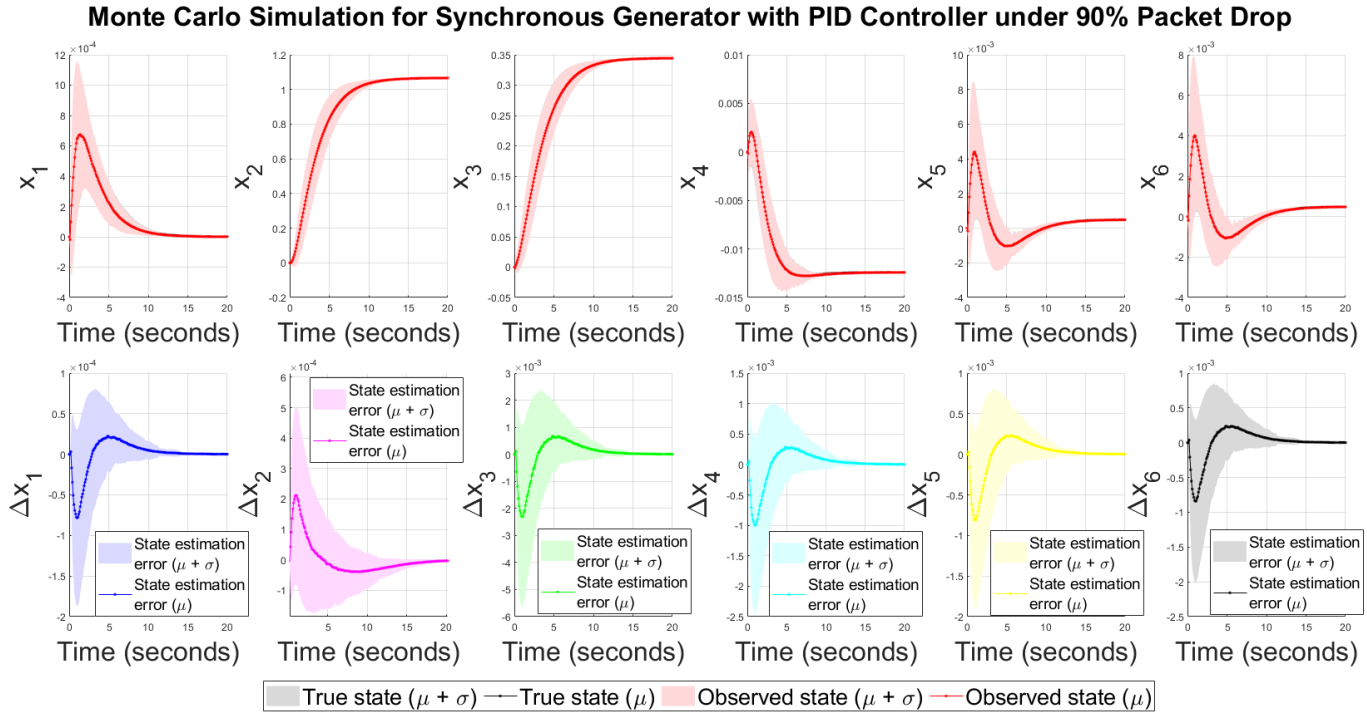

Figure 13: True/observed states and state estimation error using observer-based PID controller with 90% packet drop for the discretized model of synchronous generator with PSS.

Using these obtained gains of the observer and PI/PID controller, the state trajectories of true, observed states and the state

estimation errors are simulated with 50% and 90% random packet drop probabilities in both the feedback and forward path of the control loop for the synchronous generator which are shown in Figure 10-Figure 13. The bottom panels of the time responses show the state estimation error $\Delta\mathbf{x}_i, i \in \mathbb{Z}_+$ which should not be confused with the state variables themselves, since these are fluctuations of the state estimation error defined in (52) and hence will converge to zero.

As the second test-bench energy system, we also carried out 1000 Monte Carlo simulations to check the effectiveness of the proposed joint controller/ observer design method under 50% and 90% random packet loss probabilities. It is seen that all the states are converging to the true state trajectories with the designed observer/controller gains $\{\mathbf{L}, K_p, K_i, K_d\}$. It is evident that all the estimation errors are converging to zero with both the controllers and medium/higher packet drop cases. However, the error bands are wider for higher rate (90%) of packet drops and with the PID controller yielding higher std of the state oscillations while a much better response is obtained using the PI controller with observer. The control signals to the system using PI and PID controller are shown in Figure 14 under 50% and 90% random packet drop in the feedback and forward path of the control loop. Similar to previous case, a high control effort is required for the larger packet dropout case, as evident from large oscillations in the control signal for a longer time ~10 sec. For the 50% packet drop case, with both PI/PID controllers the oscillations in the control signals damp out very fast i.e. within 1.5 sec.

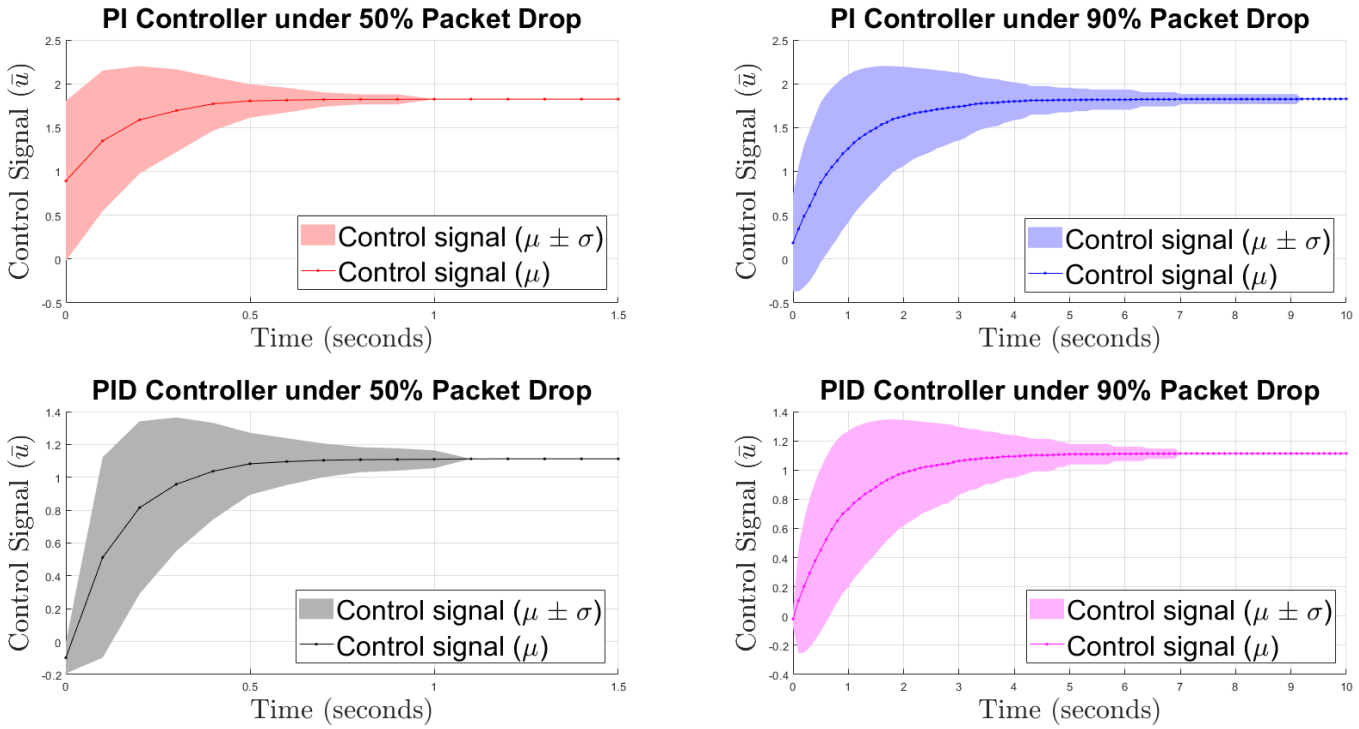

Figure 14: Control signal using observer-based PI and PID controller under 50% and 90% packet drop for the discretized model of synchronous generator with PSS.

4.3 Discussions

Most of the efficient energy generation and conversion systems will require an open communication infrastructure and it is a challenge to integrate distributed computing, communication, and control for real time operations. However, there will be inevitable random communication delays and packet drops in the control loop due to the physical distances between the sensors, controllers and actuators [4], [5]. Previously, control laws for the energy systems like DC/DC converters and synchronous generators under communication delays and packet drops have been designed in [44], [45] but without using observer and controller with memory. However, in large scale monitoring scenarios measuring all important state variables may not be feasible due to physical and engineering constraints. Therefore, it is important to incorporate observers which can estimate the unmeasured states and enhance the monitoring and control performances of the energy systems under random packet drops due to the imperfect network effects. The proposed design method advances the state-of-the-art control design methods for these two test-bench energy systems by showing a much robust design method within the NCS framework under high specified rate of packet dropout. Our simulation results show a performance degradation for both the energy systems due to increased rate of packet dropouts, but the system stability has been maintained due to the powerful LMI method which has been validated by 1000 Monte Carlo simulations of random packet losses.

5. CONCLUSIONS

We have developed a QoS aware joint observer and PI/PID controller design method for NCS with random packet drops using the CCL algorithm to solve resulting LMIs where the rate of packet dropout can be specified in the controller/observer design process. As test-bench systems a DC/DC converter with battery and a synchronous generator with PSS have been chosen and 1000 Monte Carlo simulations were carried out with the designed controller/observer gains to investigate the effects of moderate and high packet losses on the state estimation and closed loop system performances. The joint observer and controller design method are capable of producing satisfactory performances under high (90%) percentage of packet drops. In future, this work may be further extended by considering parametric uncertainties in the system matrices along with the consideration of external noise/disturbance inputs which needs a different LMI formulation as compared to the present one. The upper bound on packet drop rate may also be explored analytically and/or in simulations in the future since for very high packet drop rates, a feasible set of controller and observer gains may not always be found for any arbitrary test-bench system.

ACKNOWLEDGEMENT

SD was partially supported by the ESIF ERDF Cornwall New Energy (CNE), project number: 05R16P00282.

CREDIT AUTHOR STATEMENT

Kaushik Halder: Methodology, Software, Formal analysis, Investigation, Resources, Writing - Original Draft; **Saptarshi Das:** Conceptualization, Methodology, Software, Formal analysis, Investigation, Resources, Data Curation, Writing - Review & Editing, Visualization, Project administration, Funding acquisition; **Deepak Kumar Panda:** Validation, Investigation; **Sourav Das:** Software, Investigation; **Amitava Gupta:** Conceptualization, Supervision

REFERENCES

[1] X.-M. Zhang, Q.-L. Han, and X. Yu, "Survey on recent advances in networked control systems," *IEEE Transactions on Industrial Informatics*, vol. 12, no. 5, pp. 1740–1752, 2016.

[2] X.-M. Zhang, Q.-L. Han, and B.-L. Zhang, "An overview and deep investigation on sampled-data-based event-triggered control and filtering for networked systems," *IEEE Transactions on Industrial Informatics*, vol. 13, no. 1, pp. 4–16, 2017.

[3] K. Ogata, *Discrete-time control systems*, vol. 2. Prentice Hall Englewood Cliffs, NJ, 1995.

[4] W. Zhang, M. S. Branicky, and S. M. Phillips, "Stability of networked control systems," *IEEE Control Systems Magazine*, vol. 21, no. 1, pp. 84–99, 2001.

[5] J. P. Hespanha, P. Naghshtabrizi, and Y. Xu, "A survey of recent results in networked control systems," *Proceedings of the IEEE*, vol. 95, no. 1, pp. 138–162, 2007.

[6] W.-A. Zhang and L. Yu, "Output feedback stabilization of networked control systems with packet dropouts," *IEEE Transactions on Automatic Control*, vol. 52, no. 9, pp. 1705–1710, 2007.

[7] S. Hu and D. Yue, "Event-based H_∞ filtering for networked system with communication delay," *Signal Processing*, vol. 92, no. 9, pp. 2029–2039, 2012.

[8] H. Li, M.-Y. Chow, and Z. Sun, "Optimal stabilizing gain selection for networked control systems with time delays and packet losses," *IEEE Transactions on Control Systems Technology*, vol. 17, no. 5, pp. 1154–1162, 2009.

[9] A. Hassibi, S. P. Boyd, and J. P. How, "Control of asynchronous dynamical systems with rate constraints on events," in *Proceedings of the 38th IEEE Conference on Decision and Control*, 1999, pp. 1345–1351.

[10] A. Sala, Á. Cuenca, and J. Salt, "A retunable PID multi-rate controller for a networked control system," *Information Sciences*, vol. 179, no. 14, pp. 2390–2402, 2009.

[11] F. Ding and T. Chen, "Hierarchical identification of lifted state-space models for general dual-rate systems," *IEEE Transactions on Circuits and Systems I: Regular Papers*, vol. 52, no. 6, pp. 1179–1187, 2005.

[12] K. Halder, D. Bose, and A. Gupta, "Stability and Performance Analysis of Networked Control Systems: A Lifted Sample-Time Approach with L_2 Induced Norm," *ISA Transactions*, vol. 86, pp. 62–72, 2019.

[13] S. Boyd, L. El Ghaoui, E. Feron, and V. Balakrishnan, *Linear matrix inequalities in system and control theory*, vol. 15. SIAM, 1994.

[14] F. Yang, Z. Wang, Y. S. Hung, and M. Gani, "H_∞ control for networked systems with random communication delays," *IEEE Transactions on Automatic Control*, vol. 51, no. 3, pp. 511–518, 2006.

[15] Q. Zhu, K. Lu, and Y. Zhu, "Observer-based feedback control of networked control systems with delays and packet dropouts," *Journal of Dynamic Systems, Measurement, and Control*, vol. 138, no. 2, p. 021011, 2016.

[16] M. Li and Y. Chen, "Robust time-varying H_∞ control for networked control system with uncertainties and external disturbance," *International Journal of Control, Automation and Systems*, vol. 16, no. 5, pp. 2125–2135, 2018.

[17] M. Sahebsara, T. Chen, and S. L. Shah, "Optimal H_∞ Filtering in Networked Control Systems With Multiple Packet Dropout," *IEEE Transactions on Automatic Control*, vol. 52, no. 8, pp. 1508–1513, 2007.

[18] X.-H. Chang and Y. Liu, "Robust H_∞ Filtering for Vehicle Sideslip Angle With Quantization and Data Dropouts," *IEEE Transactions on Vehicular Technology*, vol. 69, no. 10, pp. 10435–10445, 2020.

[19] Y.-A. Liu, J. Xia, B. Meng, X. Song, and H. Shen, "Extended dissipative synchronization for semi-Markov jump complex dynamic networks via memory sampled-data control scheme," *Journal of the Franklin Institute*, vol. 357, no. 15, pp. 10900–10920, 2020.

[20] X.-H. Chang, Q. Liu, Y.-M. Wang, and J. Xiong, "Fuzzy peak-to-peak filtering for networked nonlinear systems with multipath data packet dropouts," *IEEE Transactions on Fuzzy Systems*, vol. 27, no. 3, pp. 436–446, 2018.

[21] Y. Wang, X. Hu, K. Shi, X. Song, and H. Shen, "Network-based passive estimation for switched complex dynamical networks under persistent dwell-time with limited signals," *Journal of the Franklin Institute*, vol. 357, no. 15, pp. 10921–10936, 2020.

[22] J. Wang, Y. Wang, H. Yan, J. Cao, and H. Shen, "Hybrid event-based leader-following consensus of nonlinear multiagent systems with semi-Markov jump parameters," *IEEE Systems Journal*, 2020.

[23] S. Santra, R. Sakthivel, S. M. Anthoni, Y. Shi, and K. Mathiyalagan, "Robust sampled-data PI controller design for networked control systems," *Journal of the Franklin Institute*, vol. 353, no. 4, pp. 797–815, 2016.

[24] K. J. Åström and T. Hägglund, "The future of PID control," *Control Engineering Practice*, vol. 9, no. 11, pp. 1163–1175, 2001.

[25] S. Dasgupta, K. Halder, S. Banerjee, and A. Gupta, "Stability of networked control system (NCS) with discrete time-driven PID controllers," *Control Engineering Practice*, vol. 42, pp. 41–49, 2015.

[26] S. Dasgupta, A. Routh, S. Banerjee, K. Agilageswari, R. Balasubramanian, S. G. Bhandarkar, S. Chattopadhyay, M. Kumar, and A. Gupta, "Networked control of a large pressurized heavy water reactor (PHWR) with discrete proportional-integral-derivative (PID) controllers," *IEEE Transactions on Nuclear Science*, vol. 60, no. 5, pp. 3879–3888, 2013.

[27] Á. Cuenca, J. Salt, A. Sala, and R. Pizá, "A delay-dependent dual-rate PID controller over an ethernet network," *IEEE Transactions on Industrial Informatics*, vol. 7, no. 1, pp. 18–29, 2011.

[28] M. Pohjola, L. Eriksson, and H. Koivo, "Tuning of PID controllers for networked control systems," in *IECON 2006-32nd Annual Conference on IEEE Industrial Electronics*, 2006, pp. 4650–4655.

[29] L. M. Eriksson and M. Johansson, "PID controller tuning rules for varying time-delay systems," in *2007 American Control Conference*, 2007, pp. 619–625.

[30] I. Pan, S. Das, and A. Gupta, "Handling packet dropouts and random delays for unstable delayed processes in NCS by optimal tuning of $PI^{\lambda}D^{\mu}$ controllers with evolutionary algorithms," *ISA Transactions*, vol. 50, no. 4, pp. 557–572, 2011.

[31] H.-D. Tran, Z.-H. Guan, X.-K. Dang, X.-M. Cheng, and F.-S. Yuan, "A normalized PID controller in networked control systems with varying time delays," *ISA Transactions*, vol. 52, no. 5, pp. 592–599, 2013.

[32] H. Zhang, Y. Shi, and A. S. Mehr, "Robust $\mathscr{H}_\infty$ PID control for multivariable networked control systems with disturbance/noise attenuation," *International Journal of Robust and Nonlinear Control*, vol. 22, no. 2, pp. 183–204, 2012.

[33] H. Zhang, Y. Shi, and A. S. Mehr, "Robust static output feedback control and remote PID design for networked motor systems," *IEEE Transactions on Industrial Electronics*, vol. 58, no. 12, pp. 5396–5405, 2011.

[34] I. Pan and S. Das, "Fractional Order AGC for Distributed Energy Resources Using Robust Optimization," *IEEE Transactions on Smart Grid*, vol. 7, no. 5, pp. 2175–2186, 2016.

[35] I. Pan, S. Das, and A. Gupta, "Tuning of an optimal fuzzy PID controller with stochastic algorithms for networked control systems with random time delay," *ISA Transactions*, vol. 50, no. 1, pp. 28–36, 2011.

[36] D. K. Panda, S. Das, and S. Townley, "Toward a More Renewable Energy-Based LFC Under Random Packet Transmissions and Delays With Stochastic Generation and Demand," *IEEE Transactions on Automation Science and Engineering*, 2020.

[37] L. El Ghaoui, F. Oustry, and M. AitRami, "A cone complementarity linearization algorithm for static output-feedback and related problems," *IEEE Transactions on Automatic Control*, vol. 42, no. 8, pp. 1171–1176, 1997.

[38] F. Leibfritz, "An LMI-Based Algorithm for Designing Suboptimal Static H_2/H_∞ Output Feedback Controllers," *SIAM Journal on Control and Optimization*, vol. 39, no. 6, pp. 1711–1735, 2001.

[39] T. Iwasaki and R. Skelton, "The XY-centring algorithm for the dual LMI problem: a new approach to fixed-order control design," *International Journal of Control*, vol. 62, no. 6, pp. 1257–1272, 1995.

[40] M. Fu and Z.-Q. Luo, "Computational complexity of a problem arising in fixed order output feedback design," *Systems & Control Letters*, vol. 30, no. 5, pp. 209–215, 1997.

[41] S. Das, S. Das, and I. Pan, "Multi-objective optimization framework for networked predictive controller design," *ISA Transactions*, vol. 52, no. 1, pp. 56–77, 2013.

[42] A. Routh, S. Das, I. Pan, and S. Das, "Stabilization based networked predictive controller design for switched plants," in *2012 Third International Conference on Computing, Communication and Networking Technologies (ICCCNT'12)*, 2012, pp. 1–6.

[43] I. Pan and S. Das, "Design of hybrid regrouping PSO-GA based sub-optimal networked control system with random packet losses," *Memetic Computing*, vol. 5, no. 2, pp. 141–153, 2013.

[44] A. Khalil, O. Mohamed, and J. Wang, "Networked control of parallel DC/DC buck converters," in *2015 IEEE Jordan Conference on Applied Electrical Engineering and Computing Technologies (AEECT)*, 2015, pp. 1–6.

[45] A. Liu and L. Bai, "Distributed model predictive control for wide area measurement power systems under malicious attacks," *IET Cyber-Physical Systems: Theory & Applications*, vol. 3, no. 3, pp. 111–118, 2017.

[46] K. Halder, S. Das, S. Dasgupta, S. Banerjee, and A. Gupta, "Controller design for Networked Control Systems—An approach based on L_2 induced norm," *Nonlinear Analysis: Hybrid Systems*, vol. 19, pp. 134–145, 2016.
[47] I. Pan, S. Das, and A. Routh, "Towards a global controller design for guaranteed synchronization of switched chaotic systems," *Applied Mathematical Modelling*, vol. 39, no. 8, pp. 2311–2331, 2015.
[48] A. K. Singh, R. Singh, and B. C. Pal, "Stability analysis of networked control in smart grids," *IEEE Transactions on Smart Grid*, vol. 6, no. 1, pp. 381–390, 2014.
[49] G. Suter and T. G. Werner, "The distribution control centre in a SmartGrid," in *CIRED 2009-20th International Conference and Exhibition on Electricity Distribution-Part 1*, 2009, pp. 1–4.
[50] L. Zhang, B. Huang, and J. Lam, "H_∞ model reduction of Markovian jump linear systems," *Systems & Control Letters*, vol. 50, no. 2, pp. 103–118, 2003.
[51] H. Gao, Z. Wang, and C. Wang, "Improved H_∞ control of discrete-time fuzzy systems: a cone complementarity linearization approach," *Information Sciences*, vol. 175, no. 1–2, pp. 57–77, 2005.
[52] H. Li, Z. Sun, M.-Y. Chow, H. Liu, and B. Chen, "Stabilization of networked control systems with time delay and packet dropout-Part I," in *2007 IEEE international Conference on Automation and Logistics*, 2007, pp. 3006–3011.
[53] H. Gao, T. Chen, and J. Lam, "A new delay system approach to network-based control," *Automatica*, vol. 44, no. 1, pp. 39–52, 2008.
[54] J. Löfberg, "YALMIP: A toolbox for modeling and optimization in MATLAB," in *Proceedings of the CACSD Conference*, 2004, vol. 3.
[55] J. F. Sturm, "Using SeDuMi 1.02, a MATLAB toolbox for optimization over symmetric cones," *Optimization Methods and Software*, vol. 11, no. 1–4, pp. 625–653, 1999.
[56] B. Hredzak, V. G. Agelidis, and M. Jang, "A model predictive control system for a hybrid battery-ultracapacitor power source," *IEEE Transactions on Power Electronics*, vol. 29, no. 3, pp. 1469–1479, 2014.
[57] A. Vasebi, S. M. T. Bathaee, and M. Partovibakhsh, "Predicting state of charge of lead-acid batteries for hybrid electric vehicles by extended Kalman filter," *Energy Conversion and Management*, vol. 49, no. 1, pp. 75–82, 2008.
[58] A. Rabello and A. Bhaya, "Stability of asynchronous dynamical systems with rate constraints and applications," *IEE Proceedings-Control Theory and Applications*, vol. 150, no. 5, p. 546, 2003.
[59] P. Kundur, N. J. Balu, and M. G. Lauby, *Power System Stability and Control*. McGraw-hill New York, 1994.